Overview of High Power Vacuum Dry RF Load Designs

A. Krasnykh

A specific feature of RF linacs based on the pulsed traveling wave (TW) mode of operation is that only a portion of the RF energy is used for the beam acceleration. The residual RF energy has to be terminated into an RF load. Higher accelerating gradients require higher RF sources and RF loads, which can stably terminate the residual RF power. RF feeders (from the RF source though the accelerating section to the load) are vacuumed to transmit multi-megawatt high power RF. This overview will outline vacuumed RF loads only. A common method to terminate multi-MW RF power is to use circulated water (or other liquid) as an absorbing medium. A solid dielectric interface (a high quality ceramic) is required to separate vacuum and liquid RF absorber mediums. Using such RF load approaches in TW linacs is troubling because there is a fragile ceramic window barrier and a failure could become catastrophic for linac vacuum and RF systems. Traditional loads comprising of a ceramic disk have limited peak and average power handling capability and are therefore not suitable for high gradient TW linacs. This overview will focus on "vacuum dry" or "all-metal" loads that do not employ any dielectric interface between vacuum and absorber. The first prototype is an original design of RF loads for the Stanford Two-Mile Accelerator.

1. *Original RF load design for SLAC linac [1, 2, 3]*

Figure 1 shows the original high power RF load (SLAC drawing: MA-767-313-01).

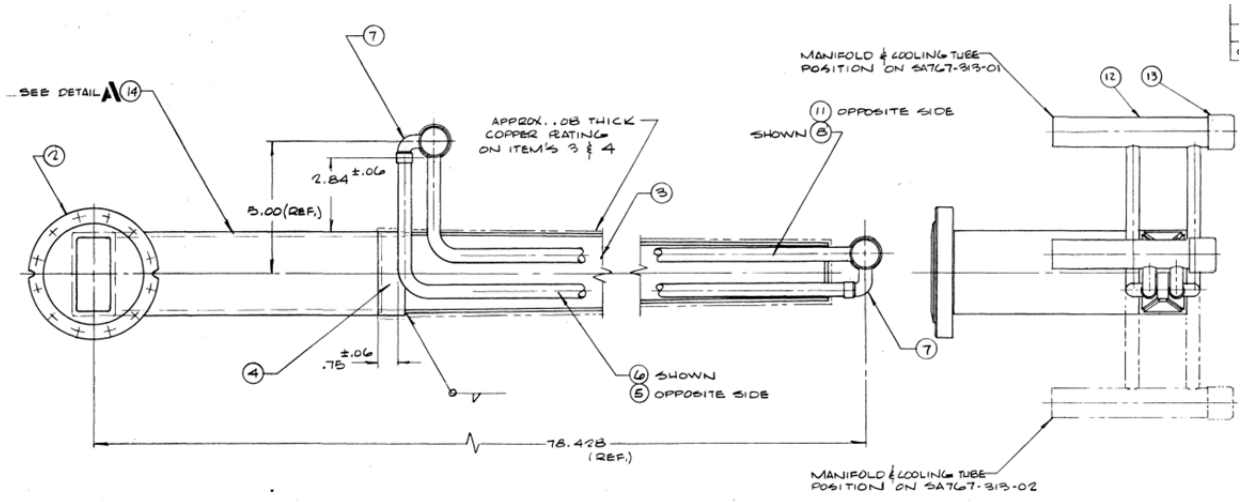

a) Main part of MA-767-313-01 drawing

This material is based upon work supported by the U.S. Department of Energy, Office of Science, Office of Basic Energy Sciences, under Contract No. DE-AC02-76SF00515.

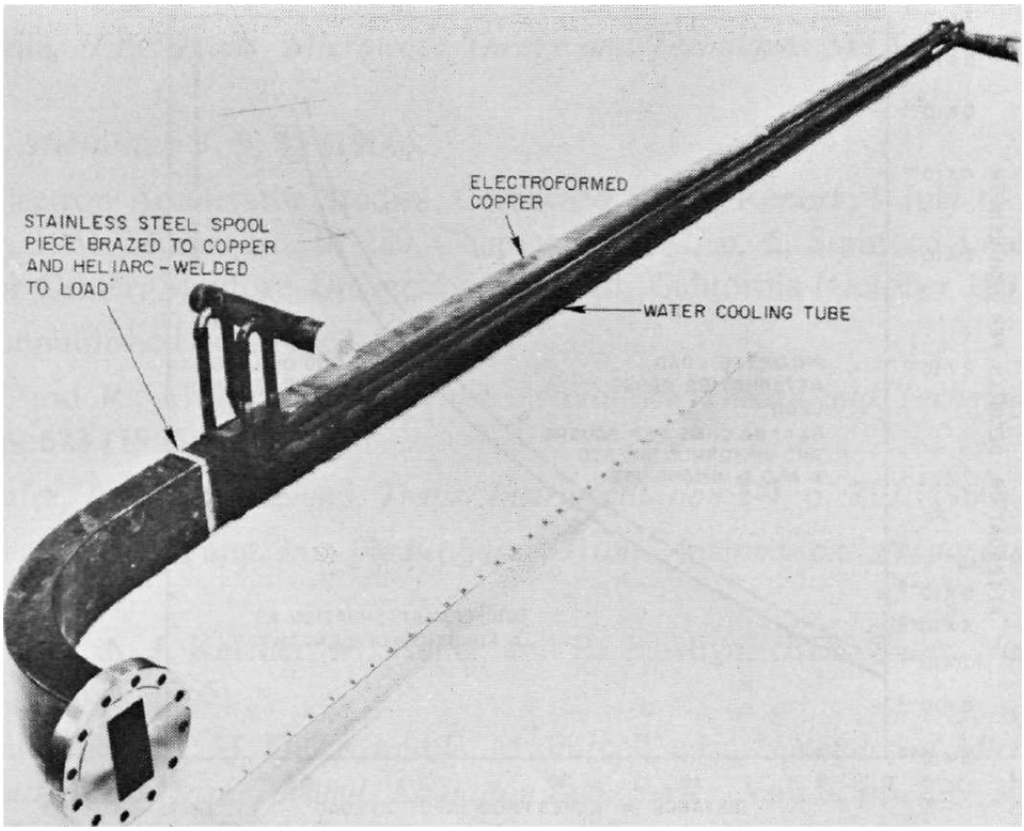

b) 3D view of SLAC vacuum dry high RF power load

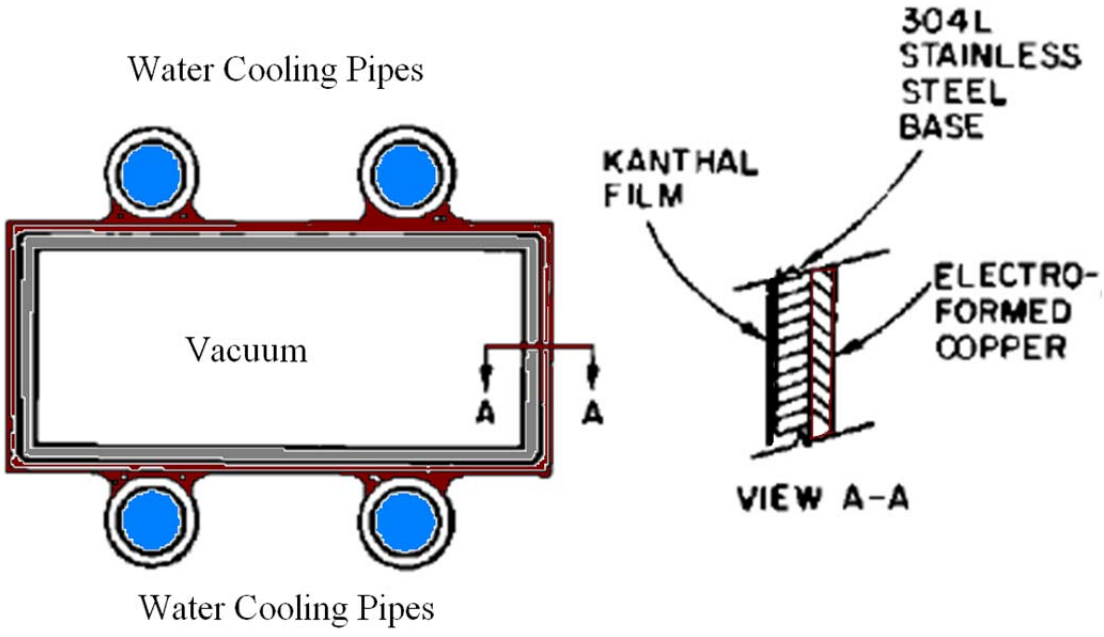

c) Cross section of the original RF load

Figure 1 Original SLAC vacuum dry load: a) Main part of MA-767-313-01 drawing, b) Load 3D view, and c) Load cross section

Original vacuum dry loads were designed to terminate 2-3 MW of peak S-Band power (see BB). There are several technological features used in the development of this RF load. Kanthal™ material is used as an RF absorbing layer. Kanthal™ is an iron based material (iron, 20-30% chromium, 5% aluminum, and traces of manganese). The stainless steel walls were prepared for welding by cleaning for UHV compatibility. These walls were sandblasted to increase the surface roughness for optimum bonding to the Kanthal™ film. Then Kanthal™ wire was flame-sprayed onto the prepared walls, except for the wall edge to be welded. The walls were tack-welded together to form a tapered waveguide channel. The final welding took place in an automatic heliarc welder to ensure a full penetration weld along the corners.

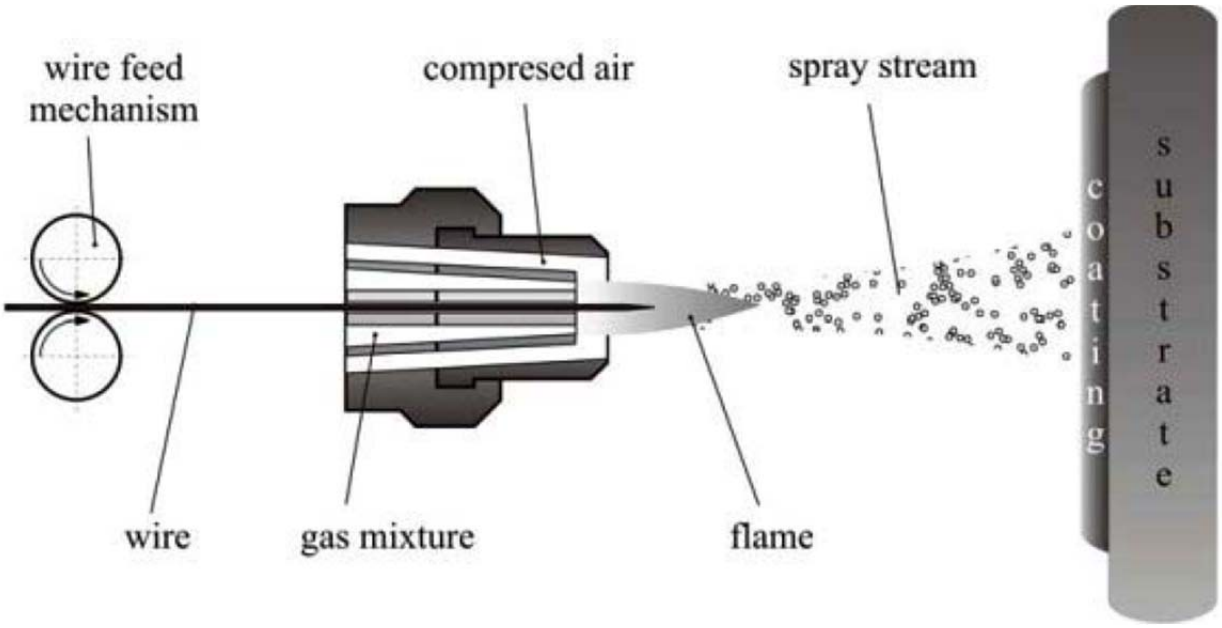

Figure 2 Flame-wire spray technology

Our experiments show that the original RF load cannot stably terminate the RF power at more than 2 MW peak. Figure 2 provides (see SLAC-WP-099) an unstable termination for the original RF load variety.

General features of flame wire spray technology is as follows. There is no deterioration or changes found on materials to be sprayed because of the low temperature spraying. The typical particle velocity spread in the spray steam is in the range from 50 to 150 m/sec. The jet temperature is approximately 3,500°K. The molten particle temperature is 2,500°C.

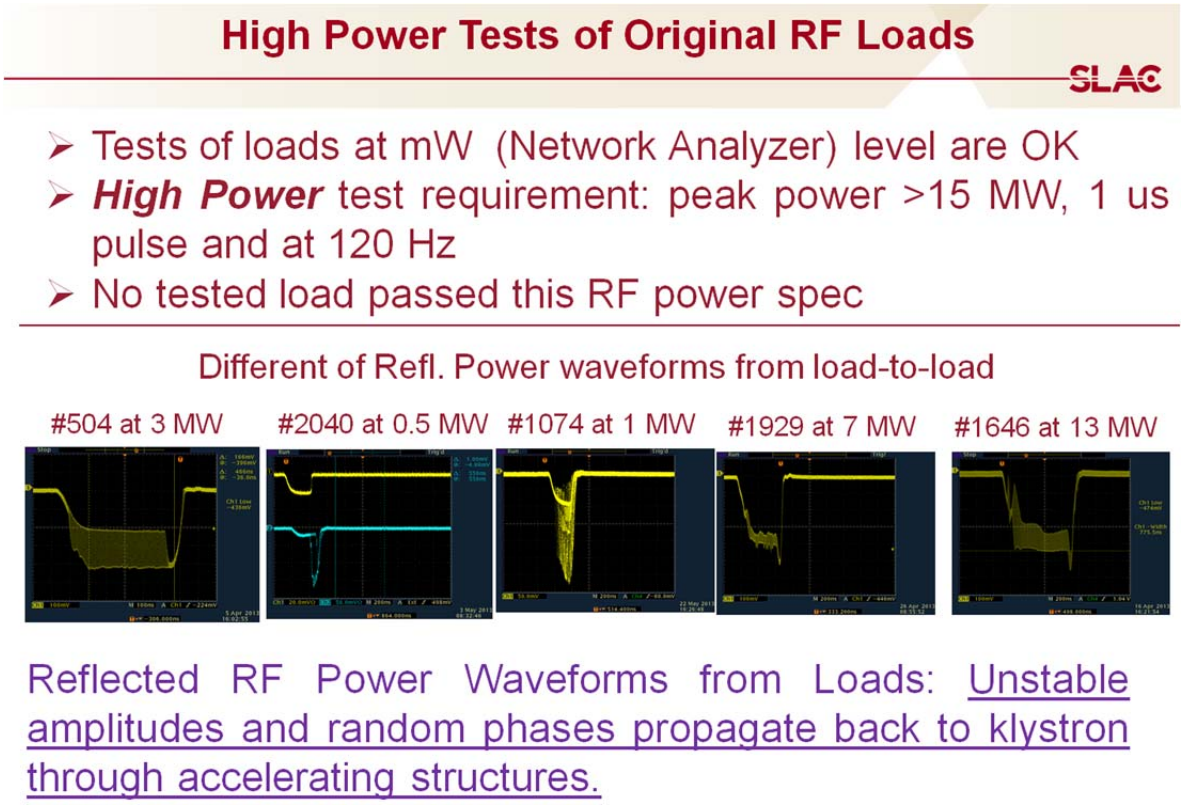

Figure 3 Illustration of unstable termination for the original RF loads [4]

An unstable RF termination lies in a wide power range. The unstable termination is a result of RF breakdown and/or multipactor mode inside of a vacuum volume. Breakdowns and/or multipactor mode produce outgassing and sputtering of the RF absorbing layer into a vacuum envelope. There is evidence of particle contamination in the RF feeder and beam line.

The unstable RF termination at the load also results in unstable reflected RF power that propagates back to the RF source through the accelerating structure. Many stations of the SLAC linac operate in the SLED mode. There are two intervals in SLED mode operation. The first interval is storage of RF energy in the SLED cavities and the second one is a discharge of stored energy into the accelerating structures. The acceleration of the bunch is synchronized with the SLED discharge period. However a part of the RF power propagates in the accelerating structure during energy storage in the SLED cavities. This RF pre-pulse power reaches the RF load. In the case of a bad termination, the uncontrollable reflected power propagates back to the accelerating structure. A resulting accelerating field at this moment will comprise of the SLED emitted field and the unstable reflected field from the bad termination. The accelerating bunch can see both fields. Unstable power may be responsible for the noise introduced into bunch.

2. Vacuum Dry Load for Next Linear Collider Test Accelerator (NLCTA) [5]

Figure 3 shows the RF load that was cut in such a way to observe the ceramic wedges.

Figure 4 Vacuum Dry Load with lossy ceramic wedges

Those lossy ceramic wedges are brazed alongside each narrow waveguide wall. There are water cooling channels at the outside of these walls. The lossy ceramic wedges are aluminum nitride (AlN) loaded with 7% glassy carbon. The array of ceramic wedges is tapered at the front. This is a transition part of the load. After the transition there is an array with a constant thickness.

This load was design to terminate a 60 MW peak, approx. 3 kW average with 10% bandwidth at 11.424 GHz center frequency. The load did not meet the spec due to surface breakdown of wedges.

3. High Power Vacuum Dry Load based on SiC Absorbers [6, 7, 8, 9]

A similar approach was employed in upgraded RF loads for KEK 2.5 GeV electron linac. Figure 4 shows the load geometry, design approach, and cut-away view.

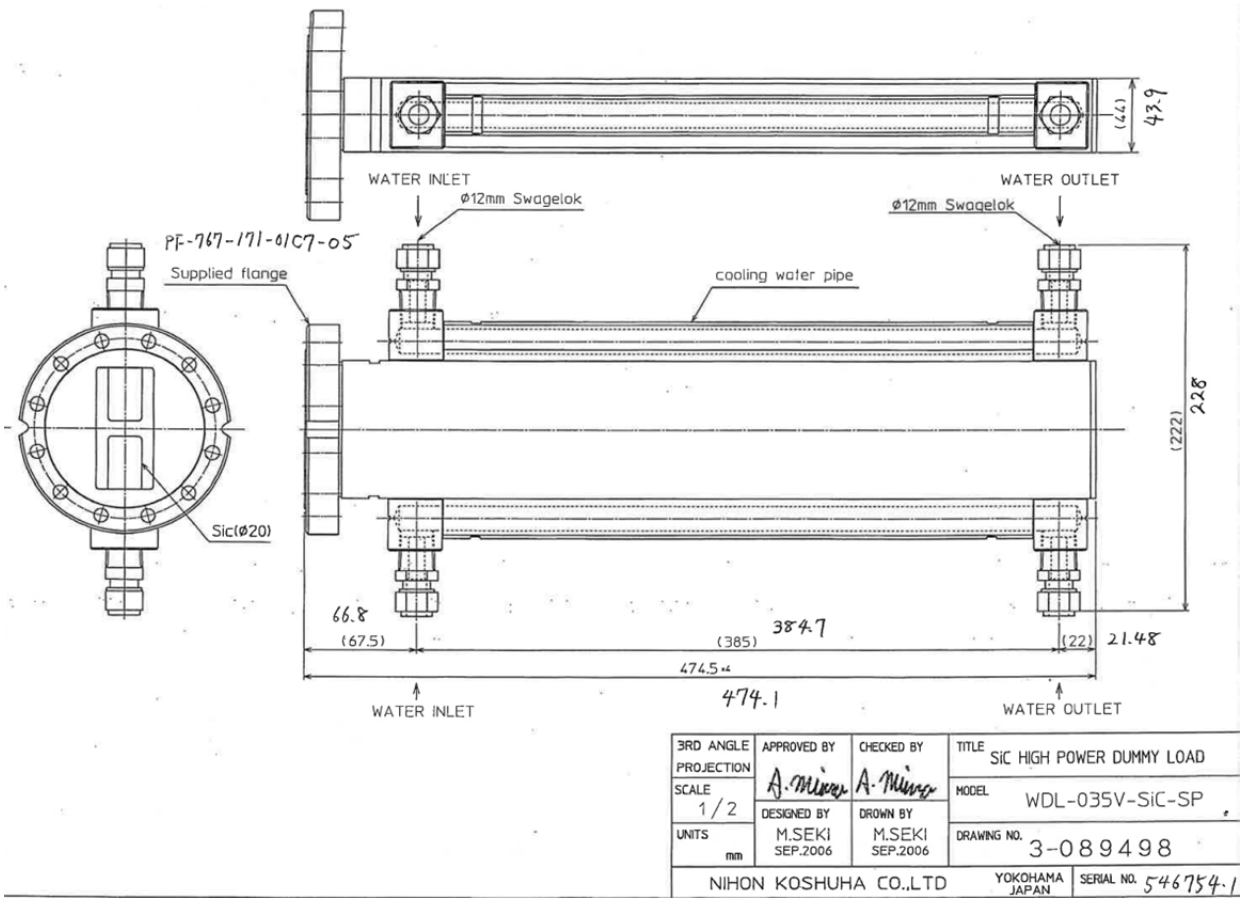
WATER INLET
ø12mm Swagelok
WATER OUTLET
ø12mm Swagelok
PF-767-171-0107-05
Supplied flange
cooling water pipe
Sic(ø20)
43.9
(44)
228
(222)
66.8
(67.5)
384.7
(385)
(22)
21.48
474.5
474.1
WATER INLET
WATER OUTLET
3RD ANGLE PROJECTION
APPROVED BY
CHECKED BY
TITLE SiC HIGH POWER DUMMY LOAD
SCALE 1/2
MODEL WDL-035V-SiC-SP
DESIGNED BY M.SEKI SEP.2006
DRAWN BY M.SEKI SEP.2006
UNITS mm
DRAWING NO. 3-089498
NIHON KOSHUHA CO.,LTD
YOKOHAMA JAPAN
SERIAL NO. 546754.1

a)

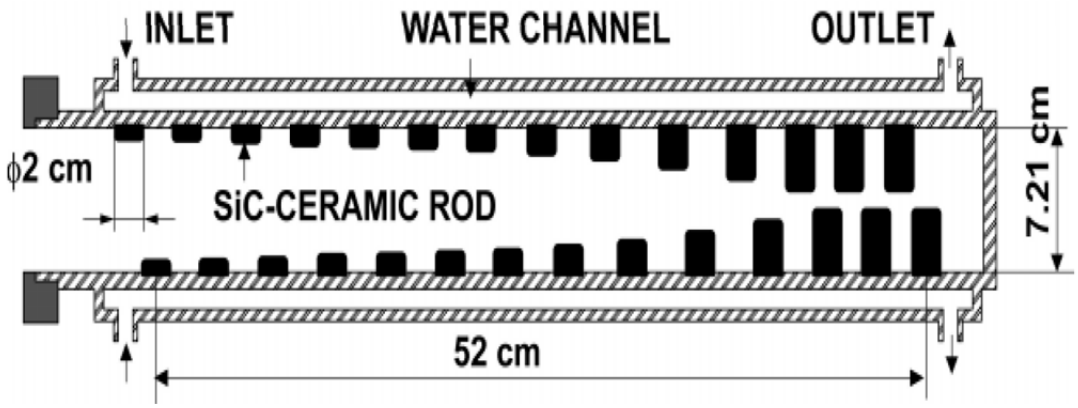
INLET
WATER CHANNEL
OUTLET
ϕ2 cm
SiC-CERAMIC ROD
7.21 cm
52 cm

b)

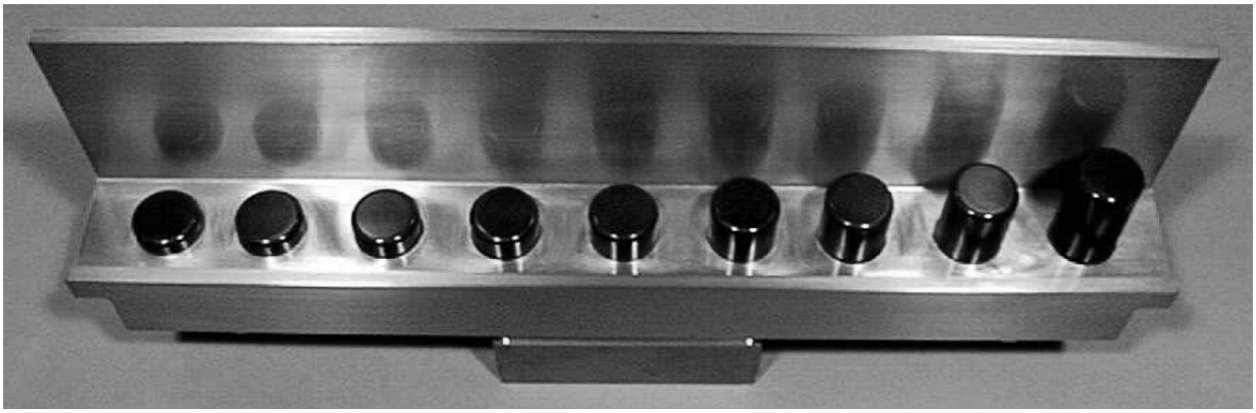

c)

Figure 5 S-Band RF load based on SiC absorber: a) Common views, b) Dry vacuum design approach, and c) Cut-away view of the E- and H- walls with the SiC posts.

High RF power is launched on the input load port and will be absorbed in the lossy SiC posts. Absorbing power converted to heat. The heat will be transmitted through SiC ceramic, braze, and waveguide wall outside of the vacuum envelope. There are two liquid cold plates which are brazed to the narrow waveguide walls. The heat will propagate to circulated water through this braze and liquid cold plate wall.

The original design contained 14 SiC posts per each H-plane waveguide wall (see Figure 5 b). The KEK linac RF load contains nine SiC posts (see Figure 5 c). Commercial available RF loads from Nihon Koshuha Co. contains eight posts only on each narrow wall (see Figure 6).

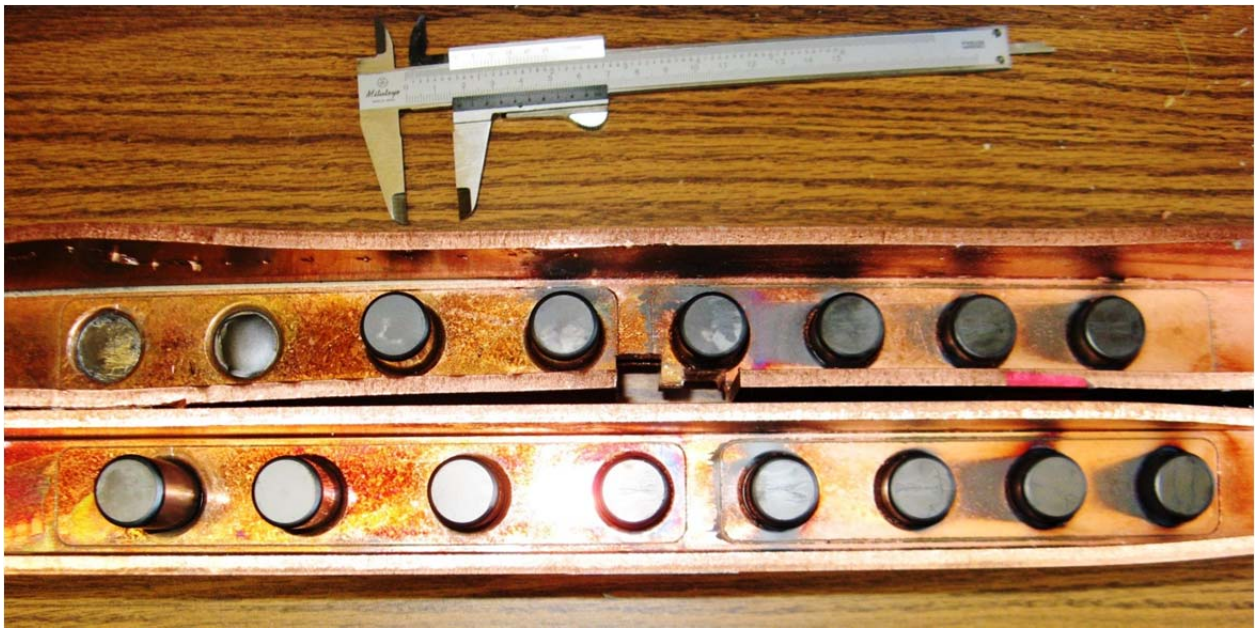

Figure 6 Cut-away view of the Nihon Koshuha Co. Dry Vacuum Load after breakdown: side by view of narrow walls

Apparently a reduction in the number of posts was done with to reduce the load cost.

Four posts are grouped per one set in the commercial load. Two sets are per one narrow wall. Four posts of each set have to be tuned to minimize the input Voltage Standing Wave Ratio (VSWR) below 1:1.1. A minimization of the VSWR denotes that only a small portion (less than 0.23% for the case above) of the RF power is reflected back from the input load port.

Posts are fabricated from SiC-ceramic samples. There are sample-to-sample variations of main SiC parameters: (1) dielectric constant and (2) loss tangent. Variations of these parameters effect load tuning and its performance. The variation of these parameters depends on the amount of sintering binders. Several steps of sintering (an evaporation of the binders) are needed to reduce the variations. A selection of individual posts with a small variation in the group is needed too. There are two major challenges in the RF load design based on usage of solid state lossy ceramics inside of a vacuumed waveguide. The first challenge is brazing of two materials with different thermal expansion coefficients. The brazing surface has to transmit a rather big heat flow. The second challenge is electrical contact and field enhancement at cooper-ceramic corners. Electromagnetic fields at sharp corners on vacuum-to-ceramic and ceramic-to-metal boundaries can easily reach a breakdown threshold if a design is poor and does not take into account a reduction of surface breakdown threshold vs. temperature.

The RF load fabrication process is expensive. It requires employment of high temperature furnaces, electrical power, and manpower. The fabrication does not guarantee that the RF loads meet a high power test because of the very gentle and long period of conditioning needed. The SiC load can be easily destroyed if there is a breakdown (or uncontrollable transients in the high power RF feeder, for example, to change linac mode of operation). For instance, Figure 7 illustrates such kind of effects.

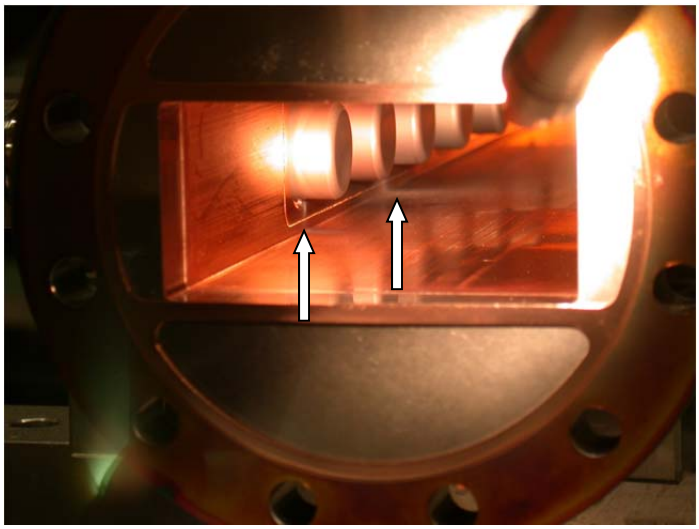

Figure 7 Breakdown signature at the SiC posts

A breakdown happened during processing at 25 MW peak, 1usec pulse width, and 120 Hz (approx. at 3 kW average). White arrows show the breakdown area. Discharge signatures are seen near first SiC posts. Dust like particles are seen in the area pointed to with white arrows after breakdown. A detail HFSS analysis (High Frequency Simulation Tool) showed that surfaces of first SiC posts are electrically overstressed. Our experience with SiC loads shows that the SiC load acceptance rate is rather low [10]. It looks like the commercially available SiC load overstressed vs. the original design where the number of

SiC posts per each narrow waveguide wall were reduced by a factor 1.75. It was confirmed by HFSS simulations. It should be noted that the surface RF breakdown on the SiC post may create discharge traces as it is shown in Figure 8.

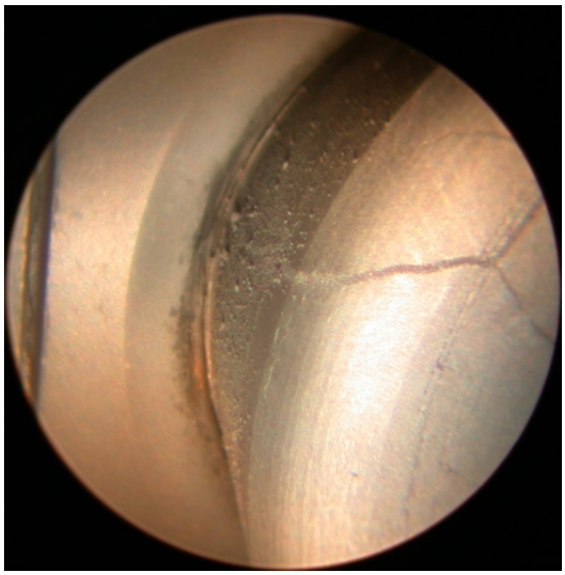

Figure 8 Arc marks on the side of the SiC post.

The RF load cannot be restored and used for a high power termination. The commercially available RF load is $11.5k (in 2006). The replacement of 320 loads for LCLS-I would be $3.2+ M (without operation cost needed for RF load conditioning).

4. RF Loads based on Stainless Steel RF Absorber [11, 12, 13, 14]

Currently we will consider two concepts.

a. Circularly polarized TE11 Loads with Stainless Steel RF Absorber

Figure 9 shows vacuum dry RF load design based on RF absorber made from stainless steel.

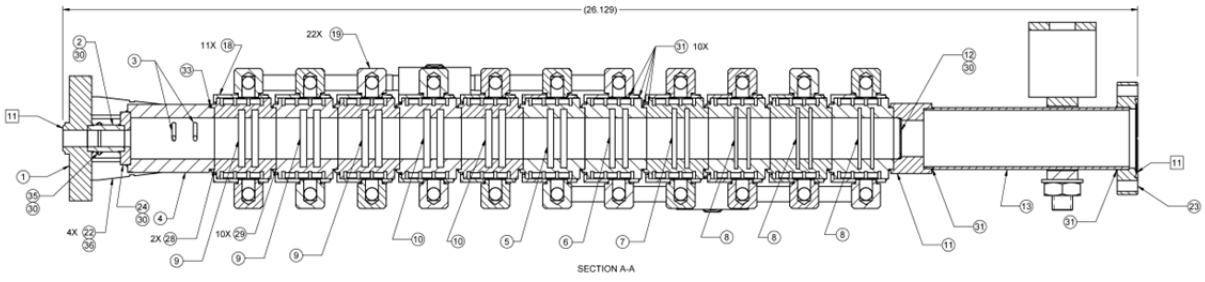

a)

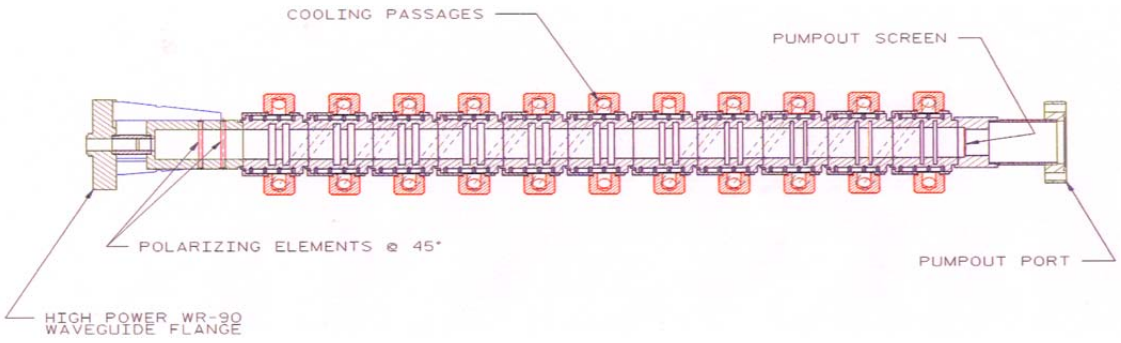

b)

c)

Figure 9 Vacuum dry load with an array of low-Q radial lines that are shorted at outer radius: a) a detailed cross section of cylindrical waveguide, b) the same cross section where functional parts are shown, and c) an assembly of four X-Band loads, which were used in experiments.

An RF power pulse is propogated in a rectungular waveguide, i.e. in a TE10 mode. However an RF termination concept is based on a lossy cilindrical approach operating in the TE11 mode. The main reason to use a TE11 mode in a cilindrivcal waveguide is to create an RF absorption that is azimuthally uniformly distributed in an array of low-Q radial lines (i.e. choks). The TE11 mode is also rotated while the RF power propagates from the input port to the load end. A circular polarizer is used at the front end of the load. The second reason to employ TE11 mode is the fact that the peak of the electric field for this mode is lower.

A pair chokes were designed in resonance (i.e. the choks deps is ~λ/4) and in such a way that the net reflection is close to zero. So, each cell consists of a pair of self- matching radial chokes made from type 430 magnetic stainless steel (SS430). The radial extent and axial length of the choke slots determine the RF power loss. A cut away of choke pair is shown in Figure 10.

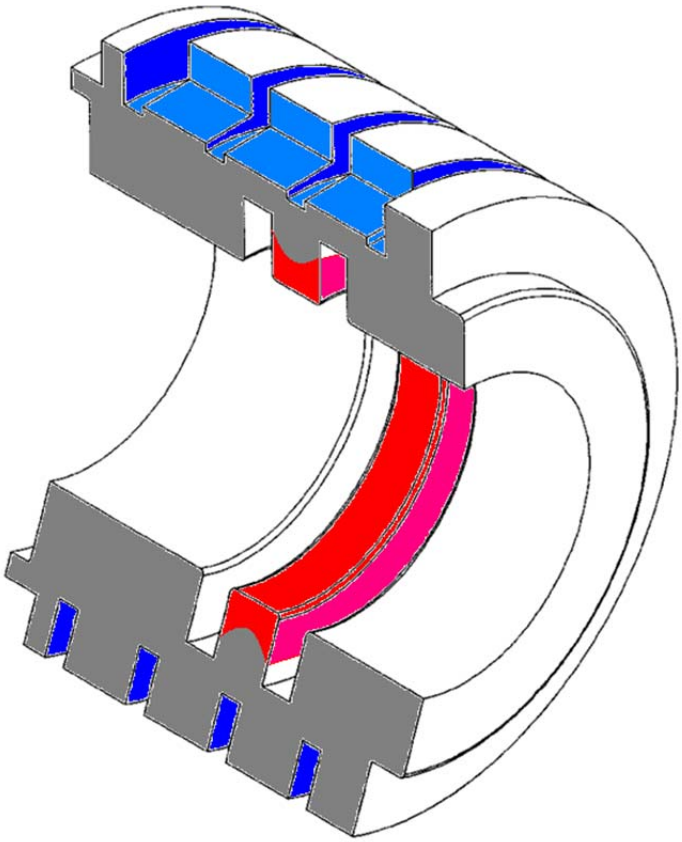

Figure 10 Cut away of choke-pair (in color). Areas with highest temperatures are colored in the red. Areas where circulated water flow are colored in blue

Sizes of each choke-pair are different from one pair to another. The thermal conductivity of SS430 is lower than SS304. However the effective RF surface resistivity of the SS304 material is lower than SS430. To get uniform power dissipation in an axial direction, the initial choke pairs are made from ss304 in the fabricated loads.

The load fabrication is costly. The design employs an array of pairs with specific dimensions. Fabricating choke pairs is a time consuming process. This load concept employs a mode converter. The RF energy is absorbed in a stainless steel layer. The heat transfer through the stainless steel is not efficient. The load assembly is complicated and requires a brazing of many parts.

b. TE10 Mode Loads with Stainless Steel RF Absorber (CERN Double Band SS430 Dry RF Loads)

Figure 11 shows the CERN Vacuum Dry RF Load.

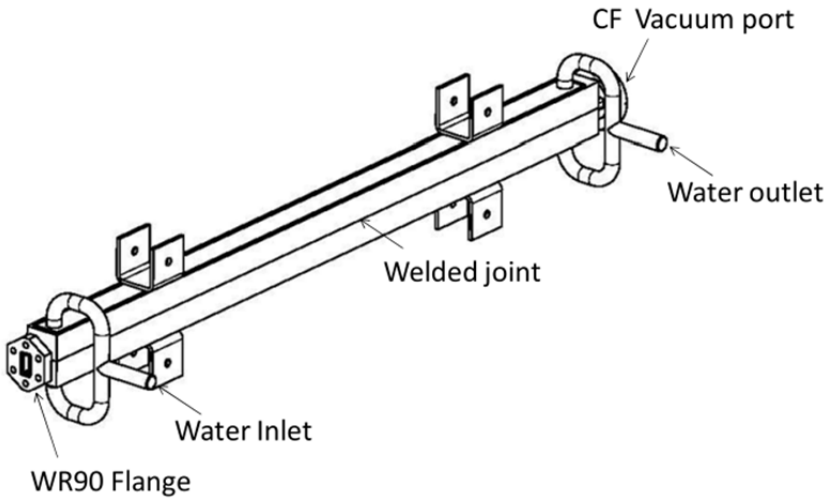

a)

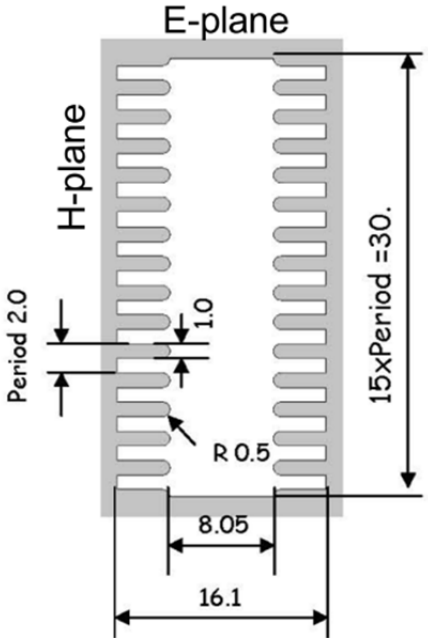

b)

c)

Figure 11 Design of CERN Vacuum Dry RF Load: a) 3D view and functionally parts, b) cross section of absorbing part made from SS430 material, and c) fabricated RF load

The whole RF load is made from SS430 material. This load consists four major parts. After a standard rectangular waveguide flange, sizes of the waveguide H-plane walls are smoothly increased. RF power is dissipated mainly on these walls at a regular part of the load. A matching section is needed between the end of the tapering and regular parts. A vacuum port is assembled on the RF load end. The regular part of the load contains an array of wedges (kerfs) on the H-plane waveguide walls. Water cooling channels are on the outer surface of H-plane walls. There are two welder joints along of E-plane walls.

The working mode is TE10 although the mode propagates in oversized taper, matching, and regular waveguide parts.

The efficiency of the RF power absorption mainly depends on two parameters: (1) surface resistivity of the SS430 steel and (2) the number and sizes of wedges. The wedges increase the effective surface resistance and attenuation rate accordingly. Due to the transition at the RF load entrance (i.e. a transition from the standard rectangular waveguide to the regular load part) the RF absorption along the whole structure is not uniform. High power RF testing shows the measured temperature of the outer surface along the welded joint at the matching section is 20°C higher than the temperature at the regular part. It should be noted that this temperature difference was measured at 0.4 kW average RF power.

The design of this load is rather simple vs. the design of the circularly polarized TE11 load although both contain additional load components (to the main part where main RF power is terminated). A labor cost of two identical waveguide walls with the wedges is less than the cost of an array of individual pair-choke cells. It should be note that a weldment is less challenging vs the brazing. Even through in the above there is a more simplified vacuum dry RF load concept that will be shown later.

The RF load design that has been considered in the above paragraph can be closest to a prototype of the new design.

4. TE10 Mode Vacuum Dry Loads with Absorber Layer based on Thermal Spray Technologies

Figure 12 shows the proposed RF load. This is a new concept. A comparison of concepts is shown in Appendix.

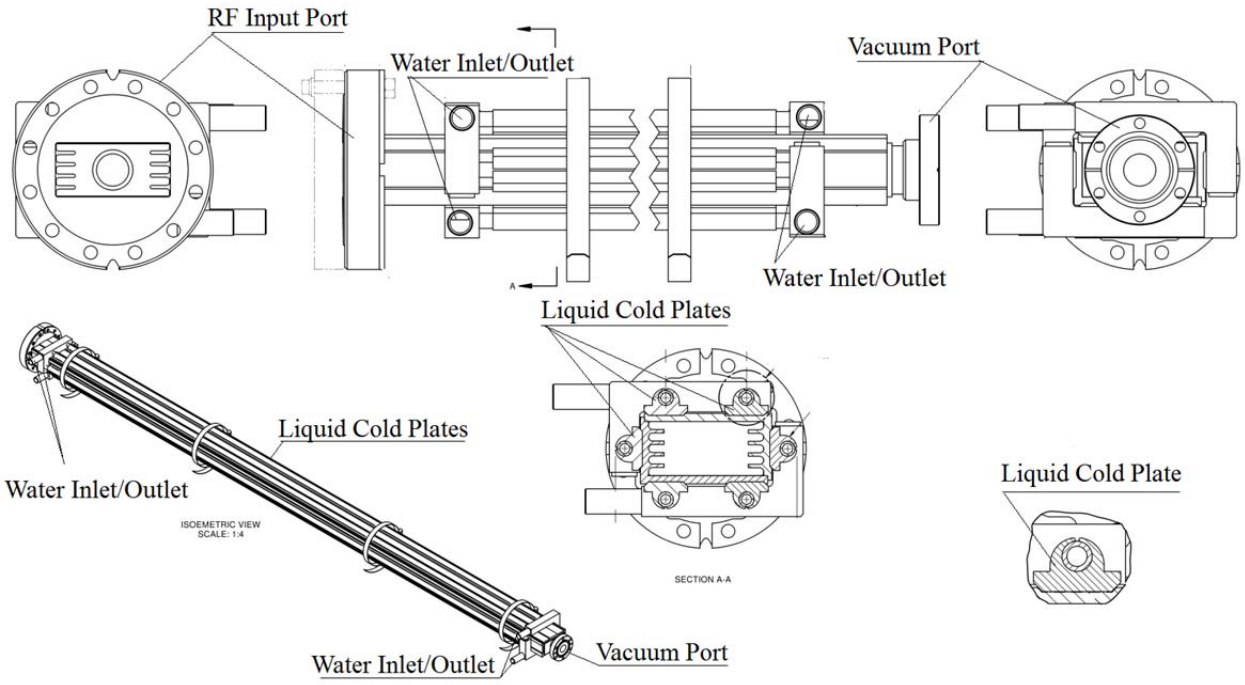

a)

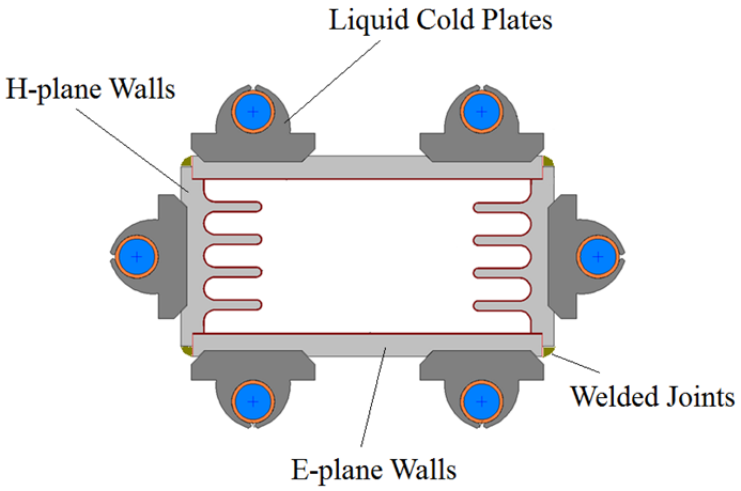

b)

c)

Figure 12 Designed RF Load: a) drawing and functionally parts, b) cross section of the proposed load, and c) fabricated RF load

The load is fabricated from four Al alloy parts. Two identical parts are E- and H- plane walls accordingly. These parts frame a channel with a standard (a x b) waveguide dimensions. The Inner surfaces of the channel are coated. Thermal spray technologies such as Electric Arc Wire Spray, Atmospheric Plasma Spray, and High Velocity Air-Fuel Spray can be employed for the formation of the RF absorber layer capable of dissipating stably and reliably a multi-MW peak (10 kW average) RF power with an acceptable UHV (Ultra High Vacuum) outgassing rate. The absorbed energy is effectively passed from the layer through the aluminum alloy wall. Coper tubes are used in the liquid cold plates.

In the proposed RF load the heat transfer materials from the absorber layer to the liquid cooling media possess higher thermal conductivity than for the materials employed in the prototypes (i.e. stainless steel).

The proposed RF load case: Heat energy is uniformly disposed on a large area of the absorber. The absorber is bonded with a substrate. A material of the substrate is aluminum alloy. A thermal conductivity of the aluminum alloy is higher than stainless steel. A reduction of the temperature allows stably working at high peak and average power.

In prototypes based on lossy ceramics, RF heat deposition is localized on a discrete volume of lossy ceramic. The heat flux is removed through the joint of lossy ceramics with the waveguide walls. The heat transfer passes through these joints. The joint surfaces are small and thermo-stressed. The lossy ceramic may be overheated. The probability for surface breakdown is higher for overheated surfaces. The RF load will be damaged and cannot be used if surface breakdown is happened.

a. An RF Absorber Material and/or matrix analysis

Kanthal™ and stainless steel (SS430) materials are widely employed as RF absorbers. Matrices of these and other materials are shown in Table 1. One can see that a matrix composition of Kanthal™ is similar to the SS430 composition except for the Al content. There is a belief that a very thin film of alumina may keep the amount of Fe and Cr components from combusting in air even at its melting temperatures. The RF surface resistivity of the absorber layer depends on this amount.

Table 1

Element Material	C	Mn	Si	P	S	Cr	Mo	Ni	N	Al
SS430	0	0	0	0	0	16	0	0	0	0
0.6	0.12	1	1	0.04	0.03	18	0	0.5	0	0
Kanthal™	0	0	0	0	0	20.5	0	0	0	5.8
1.45	0.08	0.4	0.7	0	0	23.5	0	0	0	5.8
NiCr	0	1	1	0	0	30	0	68	0	0
		1	1			30	0	68	0	0

The formation of the high peak and average RF power absorption layer requires good adhesive strength and bond with waveguide walls. Substrates are made from aluminum alloys. Aluminum alloys are preferable vs. coper for their better adhesive strength. Aluminum alloy waveguides are cheaper vs. copper. Adhesive strength and bond strength are greater than those with flame spraying.

We employ three experimentally proven thermal spray technologies and their modes for formation of a multi MW peak RF absorption layer. They are (1) Arc Wire Spray, (2) High-Velocity Air-Fuel Spray, and (3) Plasma Spray. All thermal spray technologies mention above form a good adhesive strength and bond with waveguides made from aluminum alloys.

Figure 13 shows the simplified classification of various thermal spray processes in terms of particle temperature and velocity [15].

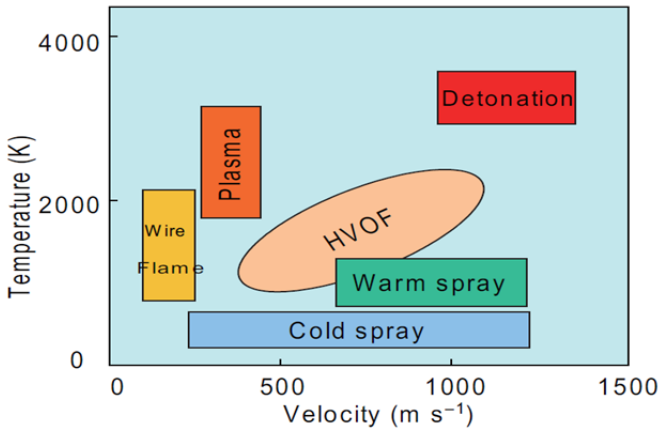

Figure 13 Simplified classification of various thermal spray processes in terms of particle temperature and velocity

In order to produce spray matrixes, all thermal spray processes require two types of energy: (1) thermal energy and (2) kinetic energy. In classical but still widely used processes such as flame spraying and wire arc spraying the particle velocities are generally low below 150 m/sec and raw materials must be molten to be deposited. However original vacuum dry loads cannot stably terminate RF more than 2-3 MW peak power where a flame Kanthal™ wire spray is used in the fabrication process. Our experiments show that there is a mode for the Arc Wire Spray technology that forms the RF absorption layer for multi MW peak power. The arc wire coated surfaces are characterized by splats that are thicker and rougher than those seen in wire flame and plasma spray technologies. The arc wire spray technology forms a higher oxide content that affects the RF absorption layer efficiency. The RF absorption rate depends on the degree of metal oxidation.

What is the best technology to form an absorbing layer capable of stably terminating the RF power at levels much higher than 2-3 MW peak? What is the RF attenuation rate in waveguide if the same media of coat is used but for different technologies? Such kinds of questions were considered in the technology development of multi MW peak and multi kW average RF loads (attenuators).

b. Description of Plasma and Arc Wire Spray Modes for Formation of MW RF Range Absorption Layers

The plasma spray technology can form the multi-MW RF absorption layer. The plasma spray technology is illustrated by Figure 14.

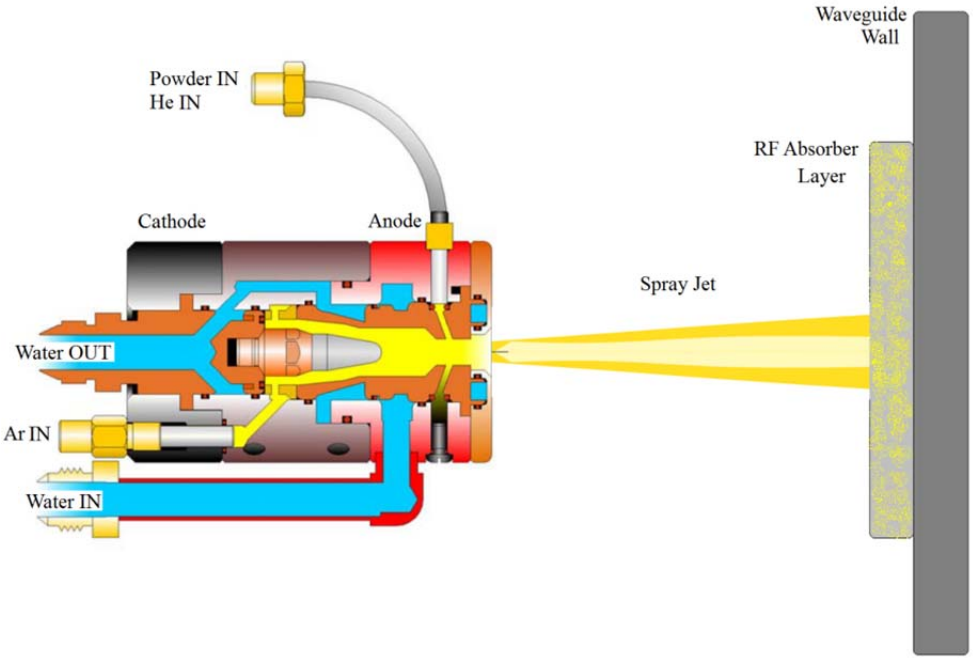

Figure 14 Plasma Spray Setup

The plasma spray process uses plasma (hot ionized gas) to melt the FeCrAl powder and propel it onto the substrate through the expanding plasma gas. Argon gas serves as the primary plasma forming

gas. Helium increases the heat content and velocity of the plasma. The plasma-arc is created between coaxially aligned tungsten cathode and subsonic anode. The gun operates on direct current from a power supply. A central control unit regulates electric power, plasma gas flow and cooling water, and sequences these parameters to initiate the process of the coat. The type of gun anode, arc current, ratio of the primary and secondary gases, and the gas flow rate control the heat content, temperature, and velocity of the spray jet. Plasma systems provide controllable temperatures that exceed the melting range of the FeCrAl matrix. The plasma spray gun setup influences the degree of particle temperature, porosity, and oxide inclusion levels and as a result on the RF features of the absorption layer. Many other gun setup parameters control particle trajectories, their speed, uniformity temperature distribution in a spray stream, etc. To form the multi-MW RF absorption layer, we employed the gun with an external powder feed. In this case particles are injected after the plasma jet leaves the nozzle and begins to expand. The particle velocity from the SG-100 plasma gun can be set in terms of subsonic, MACH I, and MACH II by different nozzles. To form the multi-MW RF absorption layer, we employed the subsonic gun setup.

A comparison of the RF properties (surface RF resistivity) shows the different result for bulk industrial FeCrAl alloy with the alloy that is fabricated by thermal spray methods. The matrix content was the same. The thermal spray produces the RF absorber with alloy splats. They are covered with oxide envelopes because atmospheric thermal spray method is used. So, the technology of RF absorption layer formation influences the RF property. Figure 15 shows one pass attenuation rate of coated waveguides for ten RF loads.

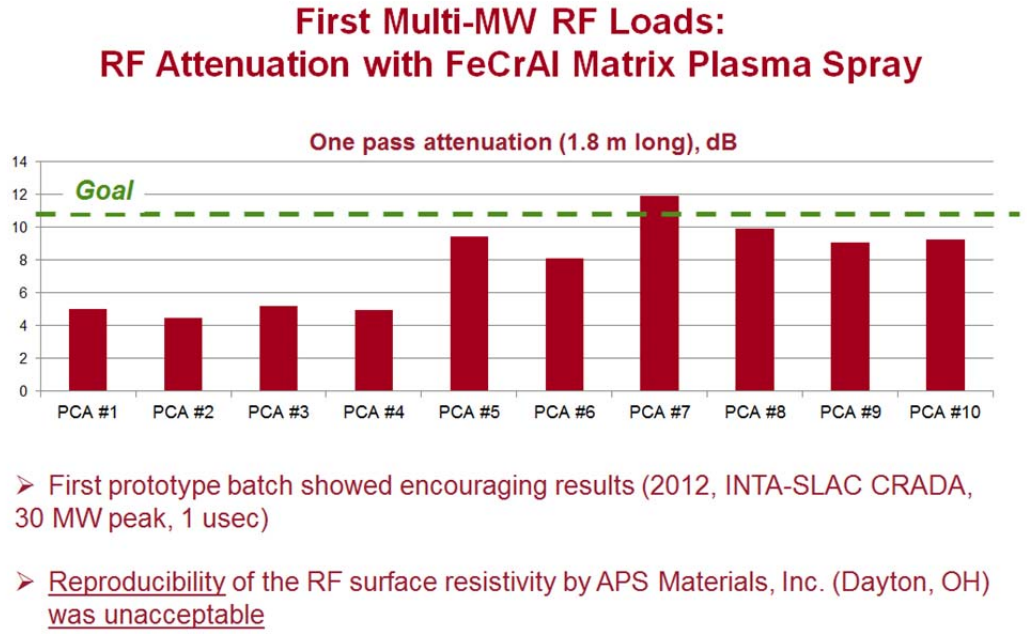

Figure 15 Reproducibility of one pass attenuation by the plasma sray technology [4]

Almost three times variation in attenuation shows that the plasma coat technology still needs to be set.

A formation of MW absorber layer is possible also by the Arc Wire Spray technology. A cross section of Arc Wire Spray is shown in Figure 16.

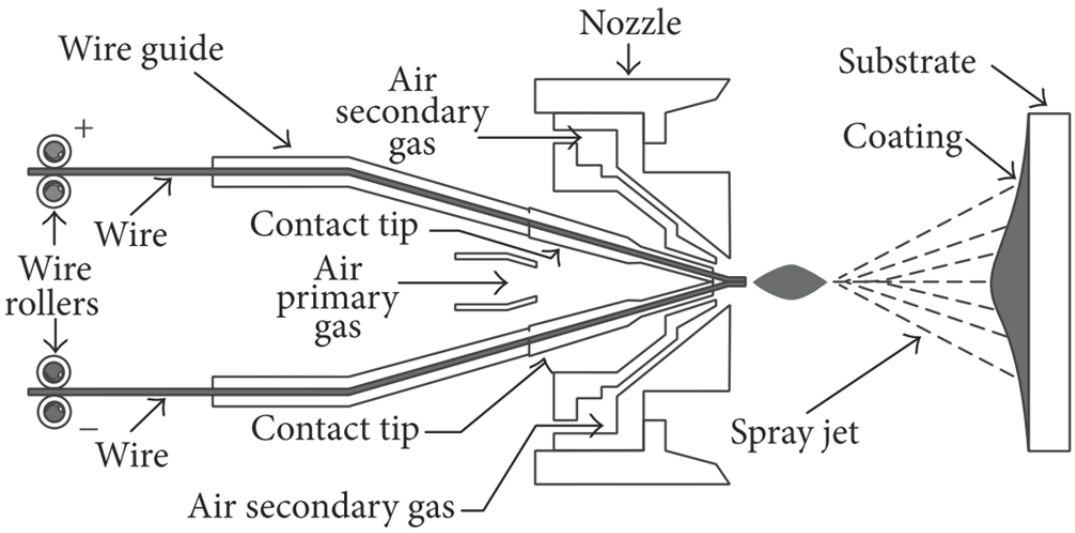

Figure 16 Common Setup/Cross Section of Arc Wire Spray Technology

The process does not require employing gases to generate the heat source. In the process two metallic wires are electrically charged with opposing polarity and are fed into the arc gun at matching controlled speeds. The wires are melted and compressed gas accelerates atomized particles onto the aluminum alloy substrate. The substrate is a part of the waveguide wall. Wire composites are shown in Table 1. In particular, the wire matrix and the spay mode by the Arc Wire Spray method for the formation of the MW peak absorption layer on the aluminum alloy walls is shown in Table 2.

Table 2

Wire Matrix	Weight, %	
	min	max
Al	4.9	5.8
Si	0.25	0.7
Cr	20.5	23.5
Mn	0.1	0.4
C	0.028	0.8
Fe	balance	balance

Mode of Electric Arc Wire Spray	Parameter
Voltage, VDC	38
Current, A	300
Air Pressure, psi	60
Air Jet Pressure, psi	18
Spray Distance, in	May be varied from 8 to 12
Robot Speed, in/min	550
Number of passes	3
Wire diameter, in	1/16
Surface preparation by a grit blast: mesh size	24
Material of Girt	Al2O3 or SiC

General features of Arc Wire Spray technology is as follows. The jet temperature is more than 25,000°K (i.e. is almost 10 times higher than the jet temperature in the wire flame technology). Typical particle velocity spread in spray steam is the range from 50 to 150 m/sec, i.e. similar to the prototype case. The molted particle temperature is higher than 3,800°C, i.e. 1.5 higher than in the wire flame technology.

Figure 17 shows surface patterns of absorber layer after technology of arc wire and plasma spray of the FeCrAl matrix.

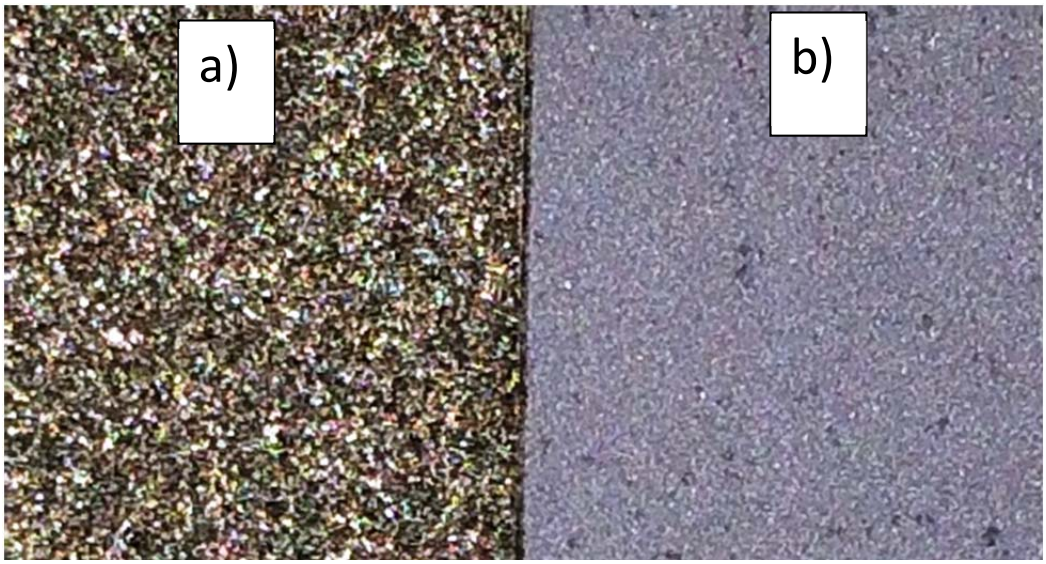

Figure 17 Surface patterns a) Arc Wire Spray and b) Plasma Spray. FeCrAl wire is used in Arc Wire Spray and FeCrAl atomized powder is used in Plasma Spray

Figure 18 shows a one pass attenuation for S-Band frequency range where different surface treatments are employed to form the multi-MW peak RF absorption layer.

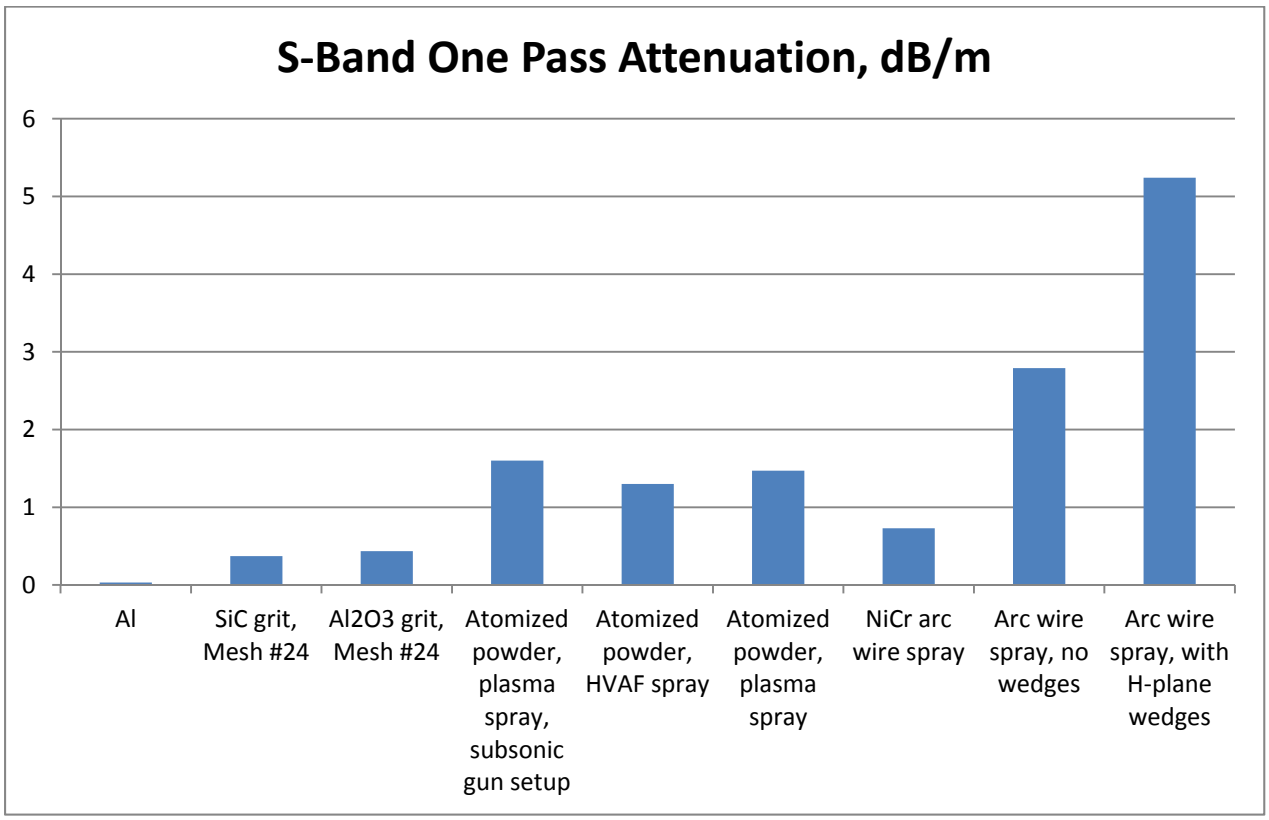

Figure 18

Arc wire spray coatings are very cost effective vs. the plasma coating. Arc wire spray also allows adjustments to achieve varied coating texture (200 micro inches – 800 micro inches). Both arc wire and plasma spray technologies forms the high RF power absorption layer.

c. Waveguide Cost and Fabrication Issues

A thousand multi-MW loads are in the SLAC linac. All these loads shall be replaced. Even taking into account the fact of replacement of the initial front end warm linac by the L-Band superconductive sections, there are potential users of the SLAC S-band components in national universities (for example, in UCLA). A reduction of unit price is one major factor in the proposed RF load concept. The price reduction dictates to focus on the simplest technical solutions. One potential solution is simple WR284 waveguide based on stock right angles. A cross section of the WR284 coated waveguide is shown in Figure 19.

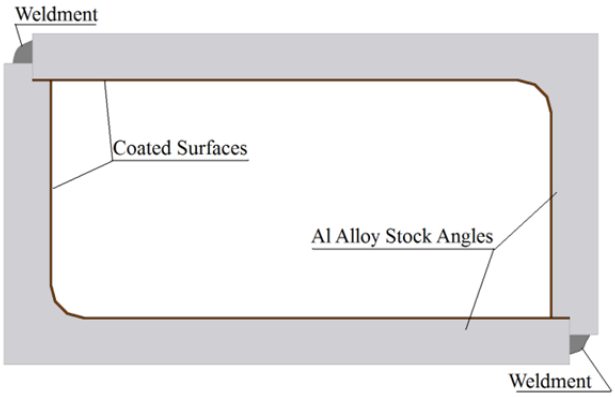

Figure 19

All conductors can be considered as bad dielectrics with high conductivity; they possess a complex dielectric constant

$$\frac{\varepsilon}{\varepsilon_0} = \varepsilon_r - j \cdot \frac{\gamma}{2\pi \cdot f} = \varepsilon' - j \cdot \varepsilon''$$

where ε' and ε" are the real and imaginary parts of the complex dielectric constant, γ=α+jβ is a propagation constant of the wave, and ω=2πf is the angular frequency. In bad dielectrics, the displacement current is small relative to the conductive current, which is the reason the real part of the dielectric constant may be omitted

$$\varepsilon' \ll \varepsilon'' = \frac{\gamma}{\omega}$$

Phase and amplitude attenuation rates (β and α) for an electromagnetic wave in the conductive media become almost equal

$$\alpha \simeq \beta \simeq \sqrt{\frac{\omega \cdot \gamma \cdot \mu'}{2}}$$

where μ' is the real part of a magnetic permeability of the conductive media. Free electrons of the RF absorber create currents when an electromagnetic wave launches on the absorber surface. These currents induce electromagnetic fields, which compensate the fields of the incident wave. A convenient way to express the conductive losses in terms of quantity δ is called the "skin depth" and is defined by the following expression

$$\delta = \sqrt{\frac{2}{\omega \cdot \mu_0 \cdot \mu' \cdot \sigma}}$$

where σ is an RF conductivity of the absorber. We shall stress that the RF conductivity value here is always different from the DC (direct current) conductivity. All free electrons of bulk material participate

in the electro conductivity for the DC case. This is not applicable for the RF conductivity. As can be seen from the expression above, the S-band electromagnetic wave penetrates the conductive absorber media only a few tens of micro millimeters deep. The rest of the free electrons do not participate in the conductivity.

A surface resistance (very often referred to as characteristic resistance) Rs is a material RF parameter that is related to its skin depth δ and conductivity σ by the following equation

$$R_s = \frac{1}{\delta \cdot \sigma} = 10.88 \cdot 10^{-3} \cdot \sqrt{\left(\frac{10^7}{\sigma}\right) \cdot \frac{1}{\lambda}}$$

where λ=cf is the free space wave length in meters and σ dimension is S/meter.

Due to the skin effect, the technology of the absorbing surface plays an important role in the value of RF conductivity. The technique of surface preparation and its roughness are essential parameters that will determine efficiency of the RF power absorption. These facts state/establish the need for experimental measurements of the RF conductivity for potential absorber materials at a given frequency (in our case, 2.856 GHz) for the chosen technology.

A piece of WR284 waveguide with TE10 mode is used between the end of the accelerating section and the RF load in the original SLAC linac concept. TE10 mode attenuation α in Np/meter in regular WR284 waveguide (with a x b =2.84" x 1.34") is

$$\alpha = \frac{R_s}{120 \cdot \pi} \cdot \frac{2}{a} \cdot \frac{\left(\frac{\lambda}{2a}\right)^2}{\sqrt{1-\left(\frac{\lambda}{2a}\right)^2}} + \frac{R_s}{120 \cdot \pi} \cdot \frac{1}{b} \cdot \frac{1}{\sqrt{1-\left(\frac{\lambda}{2a}\right)^2}}$$

where **a** and **b** are internal waveguide dimensions.

In the ideal case, a load should absorb all incident RF power with no reflection. The waveguide length should be infinitely long. Generally a small reflection that is stable during the pulse duration is acceptable for an RF source. A graph of the conductivity vs. one pass attenuation of RF power in WR284 waveguide is shown in Figure 20. Absorber materials for UHV application with σ<500 S/m would be interesting for our case.

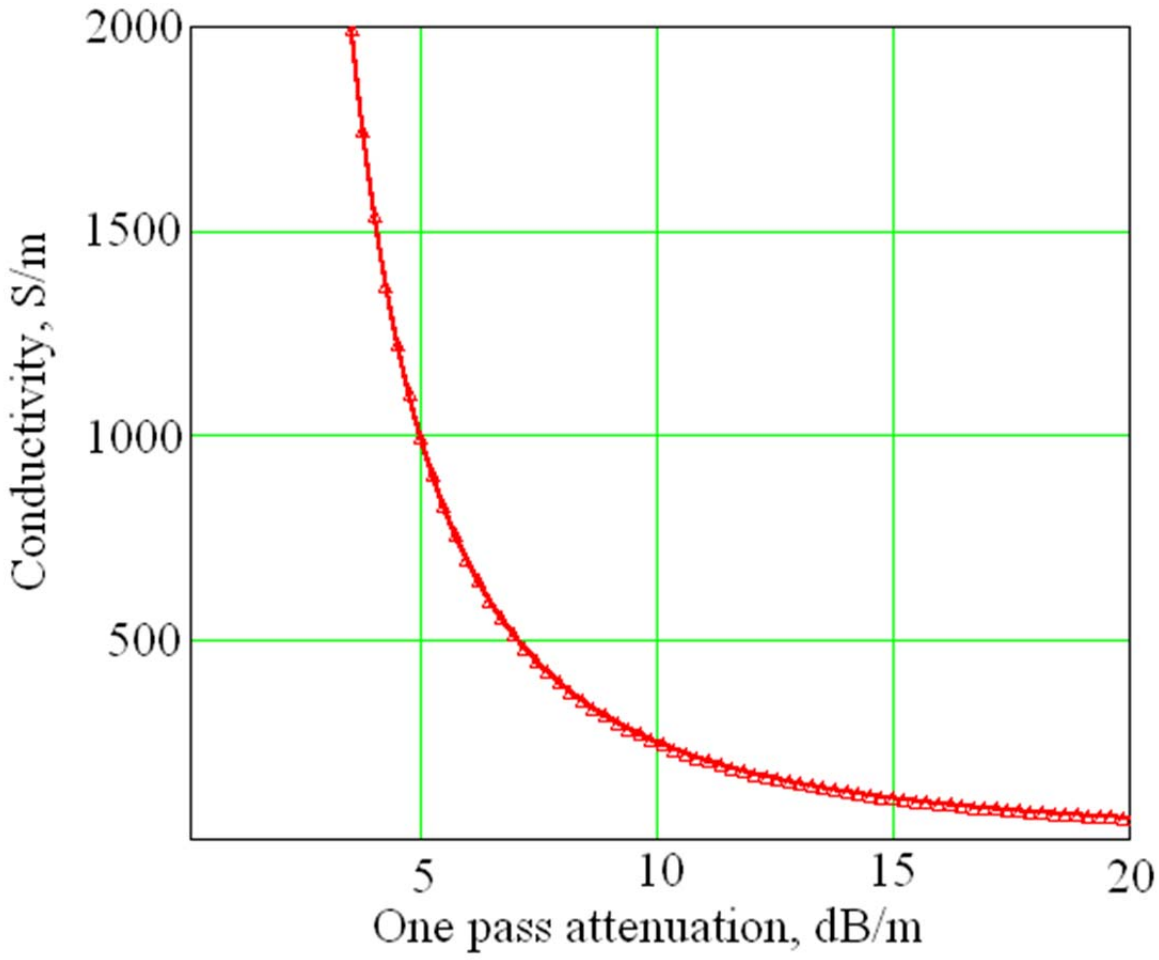

Figure 20

The minimal cost of this RF load approach mainly consists of the following components:
(1) Cost of special SS-Al transition RF flange
(2) Cost of the thermal spray on two stock right angles and waveguide fabrication cost
(3) Cost of liquid cold plates (are not shown in Figure 19).

The cost in simplest concept is approximately $4k. Cost of the thermal spray and the cost of a stainless steel to aluminum hybrid transition (an RF load input port flange) are the major cost contributors.

In this simple RF load concept, there are no matching impedance insertions, no high temperature brazing, no special extrusion of H-plane walls, no complicated and expensive mode converters are needed. However this simplest concept requires an absorption layer with surface RF resistivity of Rs=3.3 Ohm (~5 dB/m) that can stably work at multi-MW peak power in ultra-high vacuum. In this simplest and close to ideal case, the RF load can be fit in the space of the existing RF load and the existing cooling system can be used. Our technical goal is to develop the RF load close to the ideal RF load concept. Kerfs on H-plane walls are needed to get the 5 dB/m attenuation rate with lower Rs.

Summarized features of the proposed vs. the prior art technical approaches are:

- The technology employs low cost aluminum alloy extrusions. The extrusion form a part of the rectangular S-Band waveguide. Two pairs of identical extrusion parts may form a waveguide if four wall edges are longitudinally welded
- Modern thermal spray technologies and their spray modes (for example, gas pressure, flow rate, plasma gun distance against coating surface, powder feed rate, etc.) will form uniform, smooth, and dense RF absorption surfaces on the extruded parts. Instead of flame Kanthal-wire spays, the arc wire spray and the plasma spray are employed to form the RF absorption layer. These two thermal spray methods possess a higher working temperature and oxidation processes that leak differently vs. the flame spray method. A controllable automatic arm (a robot) will be employed in the spray process. An automatic spray technology allows improving the quality of a coat and its reproduction
- The RF load concept employs no tapering shape of H-plane waveguide walls. H-plane waveguide walls will be made with kerfs/wedges. An effective surface resistance is higher for a waveguide with kerfs. The size and number of wedges are optimized in such a way to get reasonable impedance matching, acceptable attenuation rate, and effective RF heat power transfer to the cooling system
- The SLAC high power RF feeders are vacuumed and traditional Skarpaas RF flanges are used for the assembly of the RF components. The Skarpaas flanges are made from stainless steel. A significant development was the introduction of a stainless steel to aluminum hybrid transition piece to accommodate the RF load end adapter flanges. There are several national companies that produce the SS-Al clad bonded plates. These plates will be machined and employed at the RF load end flanges
- Low conductive water is used inside of the SLAC linac tunnel to remove heat from different installations. All cooling channels are required to be made from the cooper. A cooper material has to be employed in the RF load cooling system accordingly. Proposed cooling channels employ cooper pipes inserted into extruded base. Six custom liquid cold plates will be placed on the modified WR284 waveguide
- Preliminary cost evaluation of proposed RF load concept is as follows. A cost of a 6 ft. waveguide from the extruded parts is less than $200 ea. A cost of the plasma spray of ferritic FeCrAl alloy on 6 ft. long waveguide is approximately $3,000. A cost of the SS-Al transition flange is approximately $1000 per each RF load. A cost for a 66” long cold plate is ~$70 per each and $420 per load. A preliminary cost per load will be 2.5-3 times cheaper against the NKC SiC vacuum dry load. Further cost reduction/optimization is possible.

Waveguide is made from four aluminum alloy parts. Parts are fabricated by extrusion method. Two parts are for E-plane and other two parts are H-plan waveguide walls. The length of parts depends on the required attenuation. Surfaces are cleaned and sand blasted before thermal spray is applied. No coated surfaces are hard masked. Parts are coated. The waveguide parts are cooled by air during plasma coat.

Figure 21 shows two sets: (1) four uncoated waveguide parts and (2) four pieces after arc wire spray.

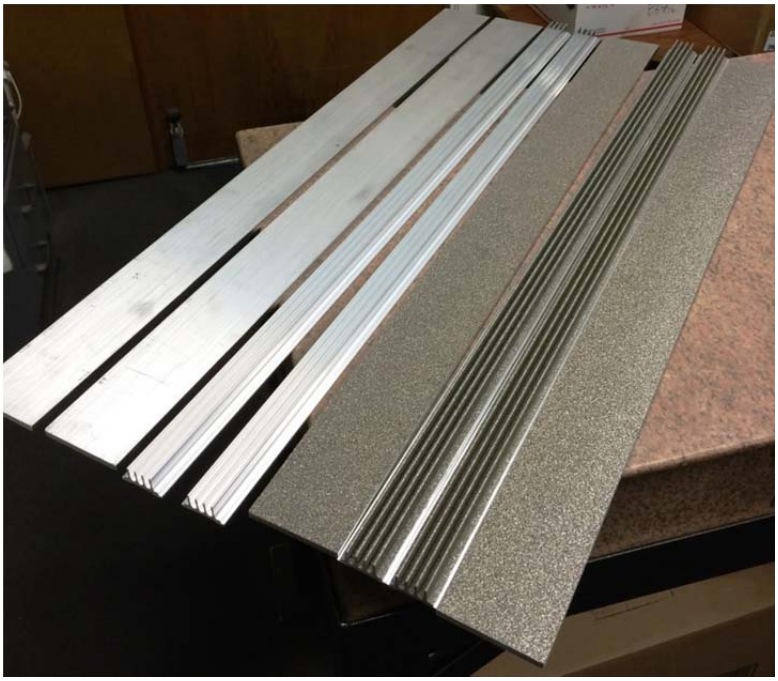

Figure 21 Uncoated and coated waveguide parts

The coated parts are assembled in waveguide and attenuation rate are checked at a low level RF power (LLRF). Figure 22 shows the assembled waveguide with an array of fixtures at LLRF lab.

Figure 22 Coated waveguide at LLRF measurement

The waveguide parts are welded. RF and vacuum port flanges are assembled. The waveguide attenuation rate is measured at a network analyzer RF power level and frequency range (see Figure 23).

Figure 23 Welded waveguide with absorption layer

Vacuum leak check and bake up are the next technological steps. After that liquid cold plates are assembled before high power tests. Figure 24 shows the installed RF load on the high RF power test stand.

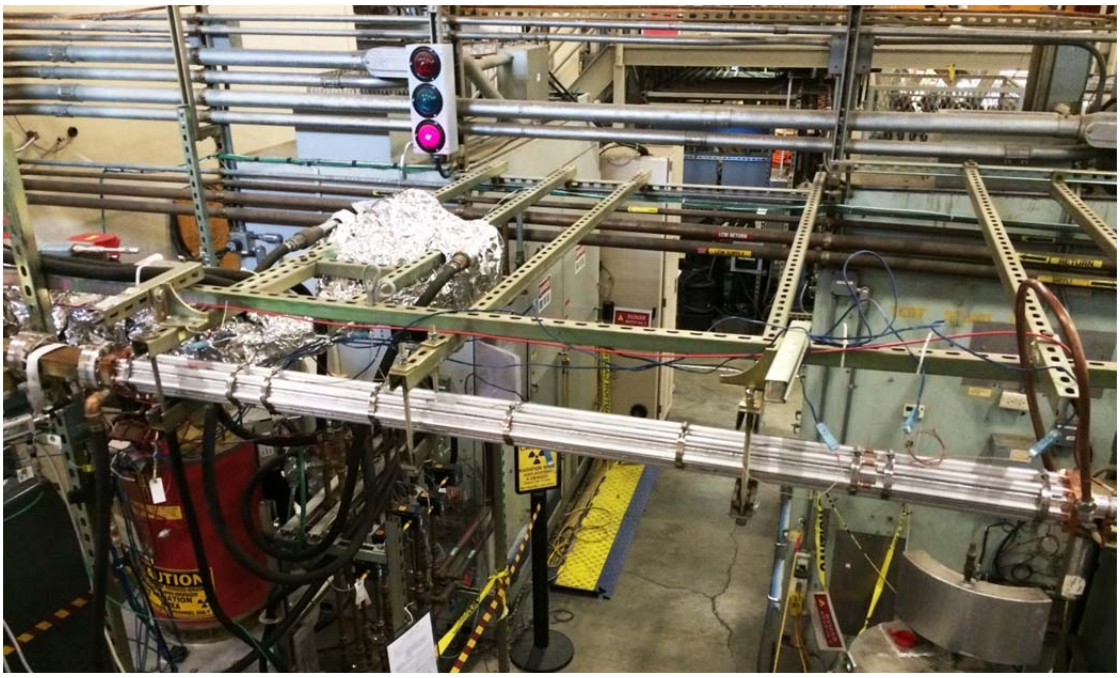

Figure 24 High RF power test stand with RF load

The stable mode of RF termination is illustrated by Figure 25 where three waveforms are shown vs. time.

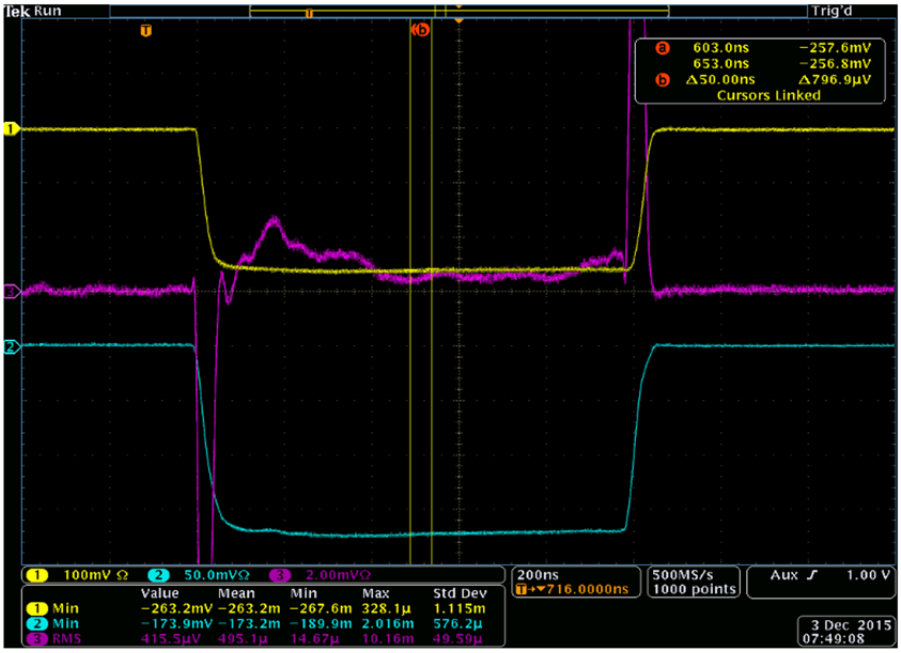

Figure 25 Waveforms of forward 32.5 MW peak (yellow trace), reflect 323 kW RF power peak (cyan trace), and a trace of the reflected phase stability vs. the input phase (magenta trace)

Amplitude of forward power is 32.5 MW peak. Reflection power is 323 kW peak. The RF load work with 120 Hz repetition rate.

Figure 26 illustrates an RF load conditioning period where the reflection power phase is unstable vs. the input phase.

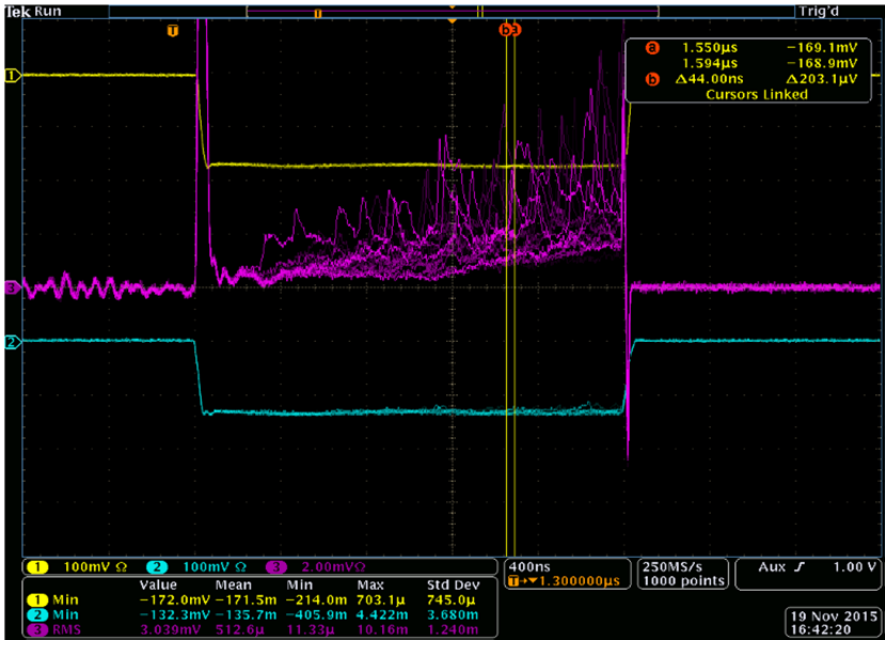

Figure 26 RF load conditioning episode shows breakdown activities inside vacuum envelope

Figure 27 shows results of partial absorber layer damage after the high RF power test.

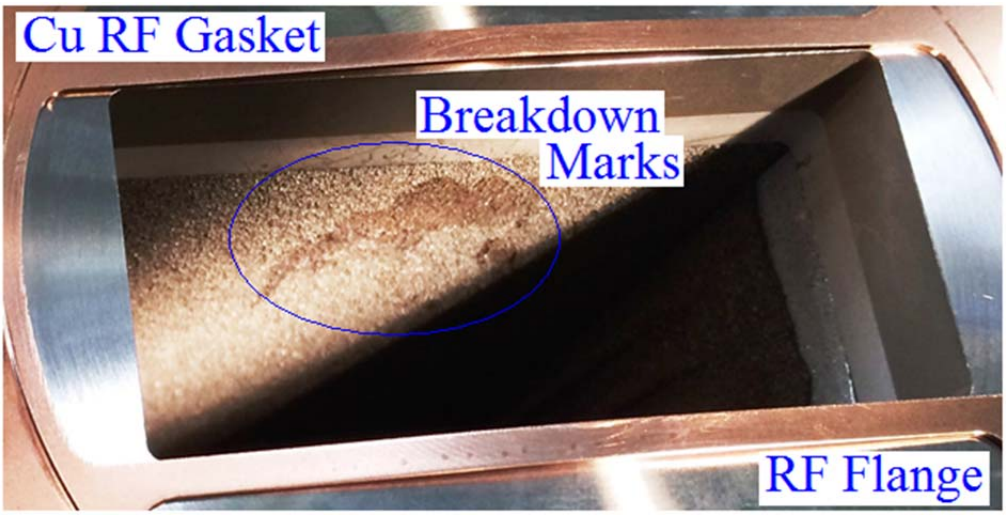

Figure 27 Area with breakdown marks is shown inside of the blue circle region (RF Load S/N 001)

However this RF load passed the high power test (30+ MW peak with a phase stable termination after the load conditioning). There was no a detectable degradation of the attenuation rate.

c. Potential Way for Further Cost Reduction

Further cost reduction/optimization is possible in the following way. Advanced high RF power load (a design only, i.e. there are no experimental results) design is shown in Figure 28.

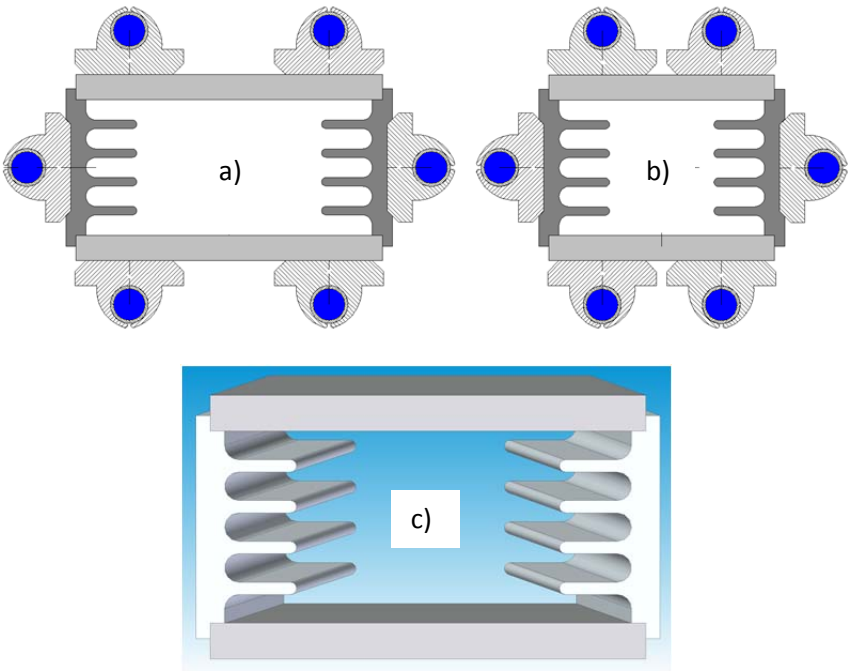

Figure 28 Cross sections of advanced RF load: a) RF entrance has a1 x b1 sizes, which correspond to the standard waveguide sizes, and b) RF end has a2 x b1 sizes where a2 = lambda/2 (lambda is a wavelength), c) 3D view

The E-plane waveguide walls (top and bottom) are tapered. There is no tapering on H-plane walls. The waveguide cross section on the end is consistent with a cutoff cross section. Modified WR284 waveguide with the tapered E-plane walls is shown in Figure 29.

Figure 29 Cross section of the RF load end is close to the frequency cutoff. Wave group velocity on this end is close to zero

Attenuation rate is varied along the waveguide as it is shown in Figure 30 for the coated modified waveguide with the tapered E-plane walls.

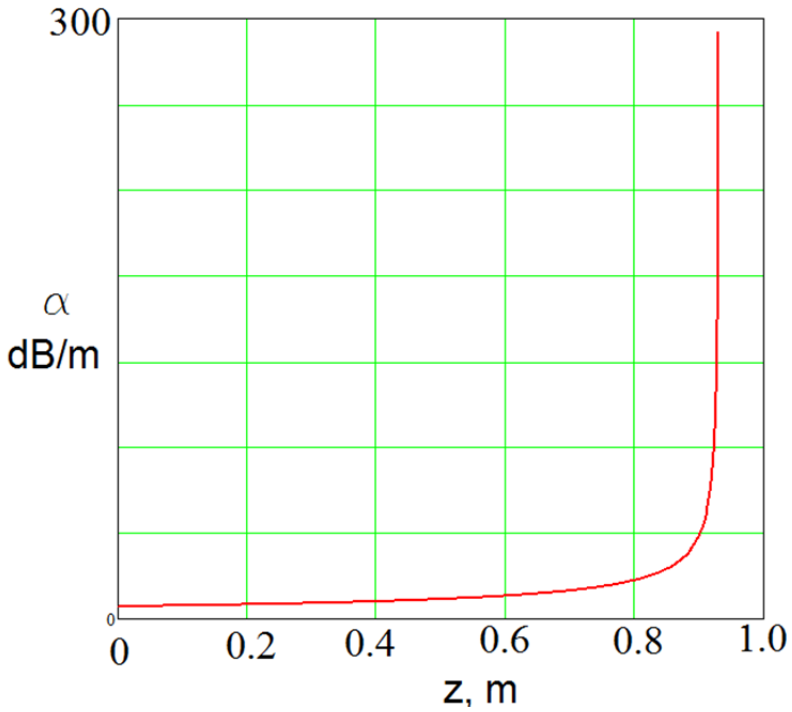

Figure 30 Attenuation rate for the waveguide with tapered E-plane walls

A calculated two way attenuation (a return loss) is -25.877 dB for one meter long waveguide with a shorted end. The result at the LLRF network analyzer is shown in Figure 31.

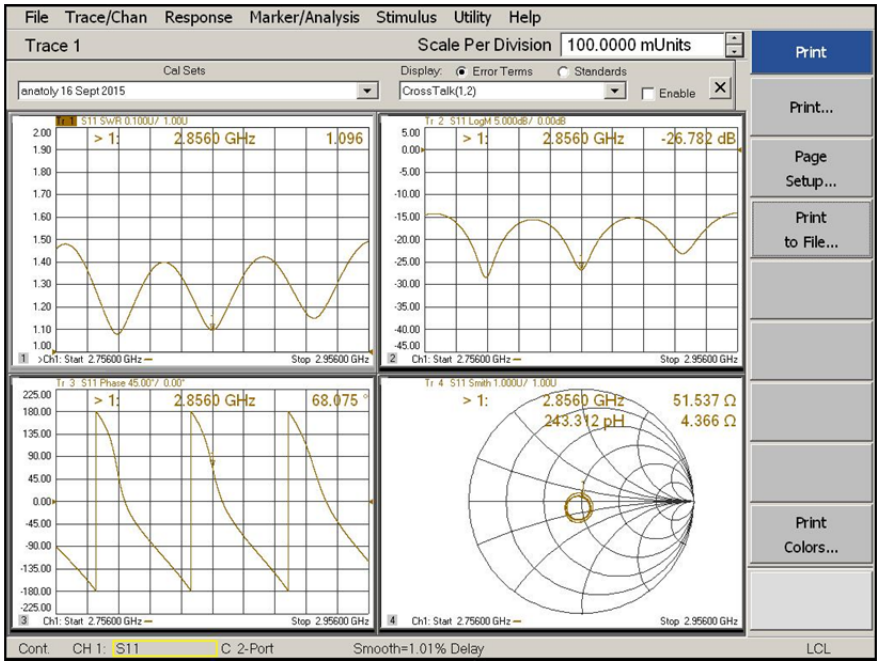

Figure 31 LLRF measurements of scatering parameter for the waveguide shown in Figure 29

One can see that s11 is -26.8 dB and close to the calculated. A high power test of the advanced RF load concept is necessary. The waveguide length is reduced approximately two times. The thermal spray cost would be reduced by the same factor. However the design will require a careful thermal stress and vacuum analysis and considerations.

The proposed RF load concept employs no tapering shape of H-plane waveguide walls. H-plane waveguide walls are made with kerfs/wedges. An effective surface resistance is higher for a waveguide with kerfs. The size and number of wedges are optimized in such a way to get reasonable impedance matching, acceptable attenuation rate, and effective RF heat power transfer to the cooling system. A tapering of E-plane waveguide walls can reduce the RF load length and get a 30% reduction of the fabrication cost.

Conclusion

An overview of multi-megawatt RF power loads is presented. This overview discusses the “vacuum dry” load concepts that do not employ any dielectric interface between vacuum and RF power absorber. A main focus of the overview is a comparison and analysis of the present RF load arts. The detail analysis of thermal spray technologies is discussed. The overview demonstrates the new method and fabrication technology.

The new developed/proposed method and fabrication technology of the RF absorber layer are capable of operating in a new power range (30+MW peak and 5+kW average in the S-Band frequency range). Methods and technology can be scaled for other frequency ranges. The developed thermal spray modes

can be used for the formation of the RF absorbers that are capable of withholding multi-MW peak power. It is stated that to the known array of surface functionality achieved with thermal spray technologies, such as: abrasive surfaces, restoration of worn surfaces, resistance to abrasive, corrosion resistance to chemical attacks, hot corrosion and erosion resistances, decorative treatments, etc. can be added the new functionality: Formation of a multi-MW RF power surface absorber layer capable of stably terminating at a rate of 5.7 dB/m.

The overview describes pilot (preproduction) RF load concept that has been designed, fabricated, and tested at 32+ MW peak, 5+kW average, and 120 Hz. The average value of VSWR for fabricated loads is 1.1 and this parameter is reproducible from one load to another. The archived parameters are met for the present RF configuration of the SLAC S-Band linac. One important feature of proposed load is self-healing: the load stays alive if an RF breakdown is happened during conditioning.

The overview describes aspects of a load fabrication. The fabrication technology employs low cost aluminum alloy extrusions. The extrusion form a part of the rectangular S-Band waveguide. Two pairs of identical extrusion parts may form a waveguide if four wall edges are longitudinally welded.

Modern thermal spray technologies and their spray modes form uniform, smooth, and dense RF absorption surfaces on the extruded parts. A controllable automatic arm (a robot) will be employed in the spray process. An automatic spray technology allows improving the quality of a coat and its reproduction. The developed arc wire spray technology shows an acceptable reproducibility of RF absorbing layers at MW power range. This technology is more cost effective vs. the plasma spray.

A comparison of vacuum dry RF Load concepts is shown the appendix tables.

Acknowledgement

Author thanks SLAC LCLS coworkers for their support. This work supported by the U.S. Department of Energy under contract number DE-AC02-76SF00515.

References

[1] “The Stanford Two-Mile Accelerator”, p. 376-381, R. B. Neal, General Editor, 1968, W. A. Benjamin, Inc., NY, Amsterdam. The source nickname is “Blue Book” (BB).

[2] A. Karp and A. Schoennauer, “ Microwave Components with a Surface Coating which Impacts a Very High RF Loss, US Patent 4,971,856, Dated by 11-20-1990

[3] A. Karp, “Microwave Physics of Flame-Sprayed Kanthal™ and Other Circuit Loss Coatings”, 1985 IEDM Technical Digest, IEEE, p. 354

[4] A. Krasnykh, et.al. SLAC-WP-099

[5] K. Ko, et. al. “X-Band High Power Dry Load for NLCTA”, Particle Accelerator Conference, 1995, Proceedings of the 1995 (Volume: 3)

[6] http://www.nikoha.co.jp/eg/egindex.html

[7] H. Matsumoto et al., " Development of the S-band high power RF load" , Proc. of the 16th Int. Linear Accelerator, Conference, Japan, 1991

[8] M. Lang and W. Hopper, US Patent 4,799,031, dated by 01/17/1989

[9] M. Lang, US Patent 4,661,787, dated by 04/28/1987

[10] A. Krasnykh, SLAC-PUB-15229, LINAC12:MOPB087

[11] S. Tantawi and A Vlieks, “Compact X-band High Power Load Using Magnetic Stainless Steel”, SLAC-PUB-6826, and US Patent #5,801,598, 09/01/1998

[12] W. R. Fowkes, et. al., “An All-Metal High Power Circularly Polarized X-Band RF Load”, PAC 1997

[13] M. Matsumoto, et. al., “High power evaluation of X-Band High power Loads”, LINAC2010, Tsukuba, Japan

[14] M. Filippova, et. al., “Engineering Design and Fabrication of X-Band Components”, IPAC2011, San Sebastian, Spain

[15] S. Kuroda et. al., Sci. Technol. Adv. Mater. 9 (2008) 033002

[16] M. Neubauer, A. Dudas, and A. Krasnykh, PAC2013

Appendix

A comparison of vacuum dry RF Load concepts is shown in the following Tables

Comparison Table of Vacuum Dry RF Load Approaches

Vacuum Dry RF Loads	RF Absorber	Features	Technology	Comments
Prior Art design (S-Band) [1] 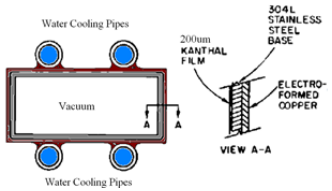	Kanthal™ -base layer in WR284 Waveguide	TE10, BW more than 200MHz, Tapered	Flame spray of Kanthal™ wire on SS base Electroform Cu layer to join the cooling pipes	2-3 MW peak Unstable termination Multipactor mode in wide power range
NKC S-Band design (S-Band) [6] 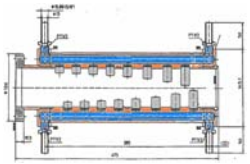	Array of SiC cylinders on H-plane	TE10, narrow BW Positions SiC necessary to be tuned experimentally at low lever RF power only	Many braze joints of SiC post with cooper plates Braze of RF flange Braze of cooling ports	<20 MW peak Overstressed surfaces of SiC posts, Long RF condition, no self-healing
CERN X-Band design (X-Band) [13] 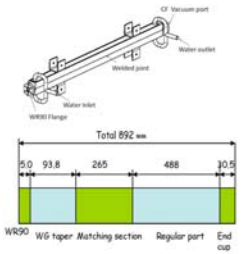	SS-430 magnetic stainless steel	11.424-12 GHz Five parts: tapering, impedance matching, absorption(regular part), and end cup (~0.9m)	Machining Welding	Length is too long (<3m) for SLAC S-Band linac Fabrication is expensive

Dry Vacuum RF Loads	RF Absorber	Features	Technology	Comments
SLAC design (S-Band) [10] 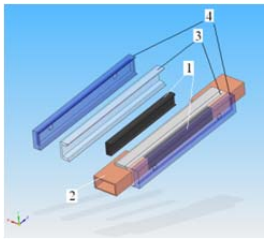	SiGraSiC	High attenuation rate, good thermal conductivity, UHV	Development of technology vacuum joint is needed Brazing	SLAC Proposal Rather expensive concept
Muons Inc. design (S-Band) [16] 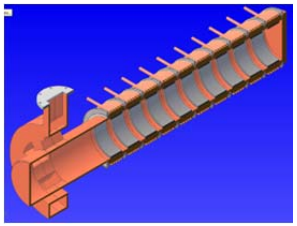	Porcelain doped by SiC powder	TE01 mode in round waveguide T10-TE01 multi-MW RF power mode converter Lossy cylinders	Lossy cylinders are mechanically confined in compression without brazing in separated cells. Cells are welded.	SLAC-Muons Inc. Proposal. Fabrication stage There is no performed a study of this concept at multi-MW RF power
SLAC design (X-Band) [11,12] 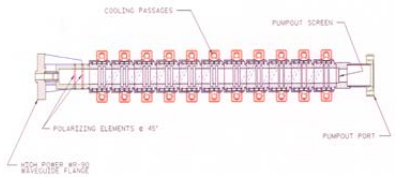	SS-430 magnetic stainless steel	Circular polarized TE11 mode in many individual RF cells Circular polarizer posts at front end	Many brazing joints of RF cells Many brazing joints of water cooling cells Brazing of polarizing posts	Labor is costly Length is too long (<3m) for SLAC S-Band linac

Dry Vacuum RF Loads	RF Absorber	Features	Technology	Comments
SLAC design (X-Band) [5] 	Lossy ceramic (Alumina Nitride and glassy carbon)	Tapering approach in ceramic bottoms	Brazing of ceramic on narrow (H-plane) side of waveguide	RF load failed with a signature of the surface breakdown on a first array of ceramic plats Expensive approach
SLAC design (S-Band) 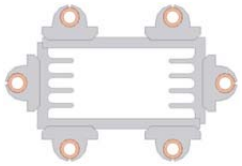	FeCrAl-base material (atomized powder or wire) as an absorber layer; plasma spray or arc wire spray technologies; spray modes are specified	TE01 Mode Broadband No tapering waveguide UHV 30+ MW peak, 5+ kW average 5+ dB/m	Thermal spray atomized size powder onto extruded aluminum alloy; plasma spray or arc wire spray technologies; spray modes are specified to handle of multi-MW peak	Cost effective technology for high power RF load and attenuators, self-healing feature

	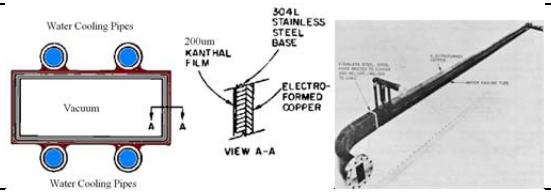	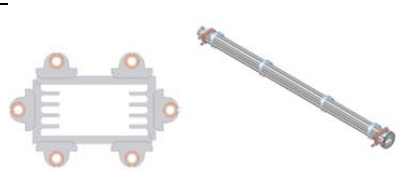
Mode of operation	TE10	TE10
Waveguide cross section	Narrow and wide waveguide dimensions are reduced along length	Only narrow waveguide dimension are kept constant along length
Wedges on H-plan waveguide walls	No	Yes
Composites of RF absorber matrix	FeCrAl	FeCrAl
Technology of absorber layer formation	Flame wire spray	Arc wire or plasma spray
Substrate	Stainless Steel	Aluminum Alloy
Level of RF power to be terminated, MW peak	2-3	30+
Stability of termination	poor	good